Atmos. Meas. Tech. Discuss., 8, 3605–3666, 2015
www.atmos-meas-tech-discuss.net/8/3605/2015/
doi:10.5194/amtd-8-3605-2015

Atmospheric Measurement Techniques Discussions
Open Access

A methodology for investigating dust model performance using synergistic EARLINET/AERONET dust concentration retrievals

I. Binietoglou[1], S. Basart[2], L. Alados-Arboledas[3,4], V. Amiridis[5], A. Argyrouli[6], H. Baars[7], J. M. Baldasano[2], D. Balis[8], L. Belegante[1], J. A. Bravo-Aranda[3,4], P. Burlizzi[9], V. Carrasco[10], A. Chaikovsky[11], A. Comerón[12], G. D'Amico[13], M. Filioglou[8], M. J. Granados-Muñoz[3,4], J. L. Guerrero-Rascado[3,4], L. Ilic[14], P. Kokkalis[5,6], A. Maurizi[15], L. Mona[13], F. Monti[15], C. Muñoz-Porcar[12], D. Nicolae[1], A. Papayannis[6], G. Pappalardo[13], G. Pejanovic[16], S. N. Pereira[10], M. R. Perrone[9], A. Pietruczuk[17], M. Posyniak[17], F. Rocadenbosch[12,18], A. Rodríguez-Gómez[12], M. Sicard[12,18], N. Siomos[8], A. Szkop[17], E. Terradellas[19], A. Tsekeri[5], A. Vukovic[16,20], U. Wandinger[7], and J. Wagner[7]

[1]National Institute of R&D for Optoelectronics, 409 Atomistilor Str., 77125, Magurele, Ilfov, Romania
[2]Earth Sciences Department, Barcelona Supercomputing Center, Centro Nacional de Supercomputación (BSC-CNS), Barcelona, Spain

Discussion Paper | Discussion Paper | Discussion Paper | Discussion Paper |

[3]Departament of Applied Physics, Universidad de Granada, Granada, Spain
[4]Andalusian Institute for Earth System Research (IISTA – CEAMA), University of Granada, Granada, Spain
[5]National Observatory of Athens, Institute for Astronomy, Astrophysics, Space Applications and Remote Sensing (NOA-IAASARS), Athens, Greece
[6]National Technical University of Athens, Physics Department, Laser Remote Sensing Laboratory, Zografou, Greece
[7]Leibniz Institute for Tropospheric Research Leipzig, Germany
[8]Aristotle University of Thessaloniki, Faculty of Sciences, School of Physics, Thessaloniki, Greece
[9]Dipartemento di Fisica, Universitá di Lecce, Lecce, Italy
[10]Èvora Geophysics Centre, Èvora, Portugal
[11]Institute of Physics, National Academy of Sciences of Belarus, Minsk, Belarus
[12]Department of Signal Theory and Communications, Remote Sensing Laboratory, Universitat Politècnica de Catalunya, Barcelona, Spain
[13]Consiglio Nazionale delle Ricerche, Istituto di Metodologie per l'Analisi Ambientale (CNR-IMAA), Tito Scalo, Potenza, Italy
[14]Institute of Physics, Belgrade, Serbia
[15]Consiglio Nazionale delle Ricerche, Istituto di Scienze dell'Atmosfera e del Clima (CNR-ISAC), Bologna, Italy
[16]South East European Virtual Climate Change Center (SEEVCCC), Republic Hydrometeorological Service of Serbia, Belgrade, Serbia
[17]Institute of Geophysics, Polish Academy of Sciences, Warsaw, Poland
[18]Institute of Space Studies of Catalonia (IEEC- CRAE), Barcelona, Spain
[19]AEMET, Barcelona, Spain
[20]Faculty of Agriculture, University of Belgrade, Belgrade, Serbia

Received: 18 February 2015 – Accepted: 16 March 2015 – Published: 8 April 2015

Correspondence to: I. Binietoglou (ioannis@inoe.ro)

Published by Copernicus Publications on behalf of the European Geosciences Union.

Abstract

Systematic measurements of dust concentration profiles at continental scale were recently made possible by the development of synergistic retrieval algorithms using combined lidar and sun photometer data and the establishment of robust remote-sensing networks in the framework of Aerosols, Clouds, and Trace gases Research InfraStructure Network (ACTRIS)/European Aerosol Research Lidar Network (EARLINET). We present a methodology for using these capabilities as a tool for examining the performance of dust transport models. The methodology includes considerations for the selection of a suitable dataset and appropriate metrics for the exploration of the results. The approach is demonstrated for four regional dust transport models (BSC-DREAM8b v2, NMMB/BSC-DUST, DREAMABOL, DREAM8-NMME-MACC) using dust observations performed at 10 ACTRIS/EARLINET stations. The observations, which include coincident multi-wavelength lidar and sun photometer measurements, were processed with the Lidar-Radiometer Inversion Code (LIRIC) to retrieve aerosol concentration profiles. The methodology proposed here shows advantages when compared to traditional evaluation techniques that utilize separately the available measurements such as separating the contribution of dust from other aerosol types on the lidar profiles and avoiding model assumptions related to the conversion of concentration fields to aerosol extinction values. When compared to LIRIC retrievals, the simulated dust vertical structures were found to be in good agreement for all models with correlation values between 0.5 and 0.7 in the 1 to 6 km range, where most of dust is typically observed. The absolute dust concentration was typically underestimated with mean bias values of −40 to $-20\,\mu g\,m^{-3}$ at 2 km, the altitude of maximum mean concentration. The reported differences among the models found in this comparison indicate the benefit of the systematic use of the proposed approach in future dust model evaluation studies.

1 Introduction

Desert dust is emitted from arid regions around the world, and in many cases it is the dominant aerosol type. Dust aerosols affect the radiation balance and temperature structure of the atmosphere by interacting both with short- and long-wave radiation (Sokolik and Toon, 1996; Pérez et al., 2006b; Balkanski et al., 2007); they also affect cloud micro-physical properties and precipitation patterns by acting as cloud condensation and ice nuclei (DeMott et al., 2003; Karydis et al., 2011) and, due to their large spatial and temporal extent, have an important effect on climate (Rosenfeld et al., 2001). The main source regions of dust are located in Northern Africa and Western and Central Asia but due to the prevalent wind patterns they have significant impact on the air quality of Europe, North America, and East Asia, far away from their sources, affecting the health of large populations (Morman and Plumlee, 2014). Additionally, mineral dust aerosols are suspected to be an important source of soluble iron in the marine ecosystems and, thus, an important factor of marine bioproduction (Mahowald et al., 2010; Nickovic et al., 2013; Gallisai et al., 2014).

Given this complexity, dust models are an important tool for studying the complete dust cycle in the atmosphere. Such models simulate dust's life-cycle including production in arid regions, transport in the atmosphere, and wet and dry deposition (Tegen, 2003). These models, which can produce complete 3-D fields of dust concentration, can be used to provide operational dust forecasts and, in total, give a bird's-eye view of dust in the atmosphere. Dust models have been used, for example, to quantify the effect of dust on air quality of Mediterranean cities (Jiménez-Guerrero et al., 2008), to study the effects of dust on weather forecasts (Pérez et al., 2006b), and to quantify the impact of lofted dust particles on cloud formation (Klein et al., 2010; Solomos et al., 2011). To perform these simulations, models rely on the physical description of atmospheric processes, on the choice of parameterization, and on the tuning of individual components in the model; consequently, modeling outputs need to be monitored against in situ and remote sensing measurements to evaluate their performance. When

AMTD
8, 3605–3666, 2015

used as a forecasting tool, models can assimliate remote sensing measurements to improve their forecasting skill (Benedetti et al., 2009; Sekiyama et al., 2010; Wang et al., 2014).

Most dust model evaluation methods are based on measurements of columnar aerosol properties. A typical quantity used is, for example, aerosol optical depth (AOD) measured by the Aerosol Robotic Network (AERONET) photometer network or satellite platforms such as the Moderate Resolution Imaging Spectroradiometer (MODIS) (e.g Pérez et al., 2011; Basart et al., 2012b). In these comparisons, the modeled dust volume concentration is converted to dust optical depth using spherical particle approximation and a modeled size distribution. These evaluation attempts are limited by the contribution of non-dust aerosols and so are restricted to cases or regions where dust is the dominant aerosol type (e.g. Basart et al., 2009; Cuevas et al., 2014).

While the columnar properties of dust are systematically studied, the vertical distribution of dust is a property that has not been explored to the same extent, even though this could have a significant effect in the total model performance. A better vertical distribution, for example, could improve the transport and removal component of the dust model and would have significant impact on the quality of the air-quality forecasts and the study of dust-radiation and dust-cloud interactions (e.g. Wang et al., 2014).

The vertical distribution of dust has been previously studied using lidar optical property profiles, but these studies have focused on few case studies (e.g. Pérez et al., 2006a; Uno et al., 2006; Müller et al., 2009; Heinold et al., 2009). Other studies have compared model optical profiles with lidar long-term observations but are limited, however, to single locations. For example, Mona et al. (2014) have presented a systematic examination of BSC-DREAM8b model dust concentration vertical distribution over Potenza, Italy, for the 2000–2012 period, using lidar-derived backscatter and extinction profiles. Similarly, Gobbi et al. (2013) compared the lidar dust extinction profiles with those modeled by BSC-DREAM8b over Rome, Italy during the 2001–2004 period. Results from both studies indicate that the dust model represented adequately the vertical distribution of dust despite underestimating the total extinction profiles.

AMTD
8, 3605–3666, 2015
Dust model comparison methodology
I. Binietoglou et al.

In this paper, we examine a strategy for cross-examining dust model vertical distribution and volume concentration profiles retrieved using lidar/sun-photometer synergy, at a continental scale. The development of advanced algorithms allows the retrieval of dust concentration profiles using the synergy of lidar and sun/sky photometer data (e.g. Chaikovsky et al., 2015; Ansmann et al., 2012; Lopatin et al., 2013) and these can be directly compared to the simulated dust distribution. Under certain assumptions, these algorithms can separate the contribution of dust from that of other aerosol types and so can be used for examining the dust model performances even in mixed aerosol cases. The retrieved dust concentration products include information about the actual aerosol size distribution – instead of relying on the model simulated size distribution – further improving the results. Up to now, the comparison of these algorithms with models has been restricted to single cases; for example, Tsekeri et al. (2013) presented a case study where the output of BSC-DREAM8b model was compared with dust concentration retrieved using the Lidar/Radiometer Inversion Code algorithm (LIRIC) over Athens, Greece, finding satisfactory agreement.

The recent implementation of LIRIC in many advanced EARLINET remote sensing stations (Chaikovsky et al., 2012) allows the systematic examination of model performance in a wider geographical region. In this paper we present a general methodology for the comparison of measured and modeled vertical dust distribution, including the strategies that could be used, the caveats that should be taken care of, and suggest the appropriate metrics that could help explore the dataset. Next, we apply this methodology to compare dust concentration profiles retrieved at 10 European remote sensing sites to 4 European regional dust transport models.

The four models that participate in this inter-comparison are BSC-DREAM8b v2, NMMB/BSC-Dust, DREAMABOL, and DREAM8-NMME-MACC. All four models contribute to the Sand and Dust Storm Warning Advisory and Assessment System (SDS-WAS) that was established by the World Meteorological Organization (http://www.wmo.int/sdswas). The SDS-WAS aims to improve the present capabilities for reliable sand and dust storm forecasts; to do this it supports the development of comprehensive, co-

AMTD
8, 3605–3666, 2015

ordinated and sustained observations and modeling capabilities of these events. The SDS-WAS consists of two Regional Nodes, one for Northern Africa, Middle East and Europe (NA-ME-E) – set in Spain – and one in Asia – set in China; each of these nodes deals with both operational and scientific aspects related to atmospheric dust monitoring and forecasting. All the models participating in the present study contribute to the NA-ME-E Regional Node.

The rest of the paper is structured as follows: in Sect. 2 we present the EARLINET and AERONET remote sensing networks, we provide an overview of the new retrieval algorithms, such as LIRIC, and present the 4 dust models used in this study. In Sect. 3 we introduce the methodology of the cross-examination, and present the appropriate statistical indicators that can be used for future evaluation of dust models. Finally, in Sect. 4 we present the results obtained by applying this methodology to real measurements. In Sect. 5 we give conclusions and indicate directions for future work.

2 Algorithms and Models

2.1 Measurement networks

The systematic observation of the vertical distribution of dust on continental scale is possible due to the development of regional lidar remote sensing networks in main dust outflow regions like the European Aerosol Research Lidar Network (EARLINET, Pappalardo et al., 2014), the AD-Net in East Asia (Sugimoto et al., 2005), the Latin American Lidar Network (LALINET) is Latin America (Barbosa et al., 2014; Guerrero-Rascado et al., 2014), and the global Micropulse Lidar Network (MPLNET, Campbell et al., 2002). This study focuses on EARLINET, a lidar network that has been established in 2000 with the aim to provide comprehensive information for the aerosol vertical distribution over Europe (Bösenberg et al., 2001). Currently, 27 stations participate actively in the network with regular contribution of data. The network includes 17 stations with multi-wavelength Raman systems, while 18 stations perform depolarization

AMTD
8, 3605–3666, 2015

measurements, giving important information on the shape of the measured particles. All stations in the network perform climatological measurements – three times a week according to a predefined measurement schedule – together with extra measurements in special events, dust measurements based on an alerting system, and intensive observational measurement campaigns (Pappalardo et al., 2014). Considerable attention has been given within EARLINET to improve and homogenize the performance of the systems, including hardware test, algorithm test on synthetic data, and system intercomparison campaigns (Matthias et al., 2004; Böckmann et al., 2004; Pappalardo et al., 2004). The optical products calculated from all the systems are stored in a standardized data format in a central database and are available for external users. The first volumes of the EARLINET database have been published in biannual volumes at the World Data Center for Climate (The EARLINET publishing group 2000–2010 et al., 2014).

Similarly, regional-to-global sun/sky photometer networks like Aerosol Robotic Network (AERONET, Holben et al., 1998), Global Atmosphere Watch – Precision Filter Radiometer network (GAW-PFR, McArthur et al., 2003), and Skyrad Network (SKYNET, Takamura and Nakajima, 2004; Kim et al., 2008) have also been developed. Many of these instruments are collocated with lidar system of the corresponding lidar networks, thus allowing the development of synergistic algorithms. In this study we use AERONET, a global network of automatic sun/sky-scanning photometers that was created in the mid 90's in order to provide global aerosol data not provided at the time by satellites and to act as a validation platform for future satellite missions. Its current aim is to provide long-term, continuous measurements of aerosol optical and microphysical properties. The network consists of standardized photometers produced by Cimel Electronique and all participating instruments undergo regular calibration and intercomparison with reference instruments. The photometers in the AERONET network perform both direct-sun and sky-scanning almucantar measurements at several wavelengths (between 340 and 1640 nm). The output of direct-sun measurements is the AOD in several wavelengths, while the sky-scanning measurements are also use

AMTD
8, 3605–3666, 2015

for retrieving aerosol microphysical properties (Dubovik and King, 2000; Dubovik et al., 2006). The processing is centrally performed and the results are made public in near-real time.

2.2 Retrieval algorithms

Different levels of lidar-based remote sensing products can be used for the evaluation of dust models, ranging from uncalibrated range-corrected signals (RCS) to dust mass concentration profiles retrieved through synergistic algorithms (Mona et al., 2012); an overview of the available lidar products is given in Table 1. The first level of products that can be used for model evaluation are range-corrected lidar signals that give qualitative information about the aerosol structure in the atmosphere (Kovalev and Eichinger, 2004); they provide an overview of dust transport processes and help check the geometrical properties of the simulated dust layers. Being almost raw lidar products, RCS can be provided even by simple lidar systems and some ceilometers (Wiegner et al., 2014; Madonna et al., 2014).

On a second level, retrieved optical properties, i.e. profiles of aerosol backscatter and extinction coefficients, give quantitative information about the total aerosol content (Klett, 1981, 1985; Ansmann et al., 1992) with well characterized uncertainties (e.g. Rocadenbosch et al., 2012); these products can be used to study both geometrical and intensive properties of the dust layers and are especially useful for optically thick lofted dust layers (e.g. Papayannis et al., 2005). They can not be used reliably, however, in cases of dust mixtures, as they do not separate the contribution of dust from other atmospheric aerosols, like smoke and pollution. In most cases no comparison can be made in the Planetary Boundary Layer (PBL) where the load of fine anthropogenic aerosols is always expected to be high, especially in most measurement sites in Europe.

If depolarization measurements are available, this problem is partly solved by a third level of analysis, which retrieves the dust backscatter coefficient profiles, based on known depolarization ratios of dust and other aerosol types (Shimizu et al., 2004;

AMTD
8, 3605–3666, 2015

Tesche et al., 2009). This allows the direct comparison of modeled dust backscatter profiles with the measured ones, without the biases introduced by other aerosol mixtures.

A fourth level of products has been developed in recent years, motivated by an increased interest in extracting aerosol concentration profiles from remote sensing measurements. Several algorithms have been developed, combining the vertically resolved lidar measurements with photometer data or assumed aerosol intensive properties; the output of these algorithms is the vertical concentration of a number of separate aerosol types.

The use of these algorithms addresses a core issue of model evaluation from remote sensing measurements: dust transport models simulate mass concentration while the main measured quantities of remote sensing instruments are optical aerosol properties; a conversion is always necessary to make the two quantities comparable. The comparison is typically done by converting the model's mass concentration to extinction profiles using an assumed or simulated volume-to-extinction ratio. If the dust transport model treats the dust size distribution in a realistic way, e.g. separating the dust concentration in many different size bins, a better conversion can be achieved using forward scattering calculations (typically based on Mie theory) on the simulated size distribution. In contrast, when using the remote sensing algorithms presented before, the retrieved quantities can be directly compared to the model output. The main benefit of this comparison is that dust microphysical properties are neither assumed a priori nor are based on model outputs, but are estimated using actual photometer measurements or measurements of pure dust types.

The existing volume retrieval algorithms fall in two broad categories. The first category uses lidar measurements and intensive optical properties of some aerosol types to retrieve the concentration of these types in the atmosphere. The used aerosol intensive properties can be derived from past observations, laboratory measurements, model data or a combination of the above. When the range of such input values is too wide for a reliable retrieval, photometer measurements are sometimes used as a proxy for the missing parameter. For example, the POLIPHON algorithm (Ansmann et al., 2011, 2012) is based on dust depolarization and extinction-to-backscatter coefficient ratio (aerosol lidar ratio) observed during the SAMUM campaign and long-term EARLINET measurements of dust transport events over Europe. In addition, POLIPHON uses the volume-to-AOD ratio derived from the photometer to approximate the variable volume-to-extinction ratio for dust and smoke aerosols. Extending this approach, Mamouri and Ansmann (2014) use laboratory measurements of fine and coarse dust depolarization ratio to further separate these two sub-classes of dust. In contrast, Nemuc et al. (2013) use properties from the Optical Properties of Aerosols and Clouds (OPAC) database (Hess et al., 1998) as a basis for their separation of dust and non-dust properties. Other approaches combining lidar measurements with airborne measurements or complex AERONET processing have also been developed (Cuesta et al., 2008; Lewandowski et al., 2010).

The second category of algorithms pursues a more tight integration of lidar and photometer data. Specifically, the retrieved volume concentration profiles are calculated by optimally fitting the aerosol concentration to the lidar and photometer measurements (Dubovik, 2005). In the case of GARRLiC (Lopatin et al., 2013), the optimal fit of the lidar and photometer measurements is found using a multi-term least square approach. Similarly, LIRIC (Chaikovsky et al., 2015) uses the AERONET inversion products to derive the intensive properties of fine and coarse aerosols; consequently, the algorithm finds the optimal profiles of these types based on lidar measurements and total-column volume concentration profiles provided by AERONET.

In this paper, we use results from the LIRIC algorithm to show the benefit of using such algorithms for dust model evaluation. LIRIC was chosen as it takes full advantage of the remote sensing networks EARLINET and AERONET, and is used by a large number of aerosol remote sensing stations in Europe (Chaikovsky et al., 2012); the results we present are, nevertheless, applicable to similar datasets retrieved by other algorithms. The details of LIRIC can be found in Chaikovsky et al. (2015) so only a brief overview is given here.

AMTD
8, 3605–3666, 2015

LIRIC assumes that the aerosols in the atmosphere, at any given moment, can be described as a mixture of few aerosol components. These are expected to have constant microphysical properties throughout the atmosphere, but with varying concentration with height. LIRIC retrieves these height-dependent concentration profiles based on AERONET microphysical inversion products and multi-wavelength lidar measurements. Aerosol intensive properties are estimated from the AERONET retrievals by splitting the aerosol size distribution into fine and coarse modes by finding its minimum concentration value in the 0.194–0.576 µm range. The intensive properties of the two modes are calculated assuming a mixture of spheres and randomly oriented spheroids. When lidar depolarization measurements are available, the coarse mode can be further separated into spherical and spheroidal parts, based on AERONET's sphericity parameter. Finally, LIRIC retrieves the component's volume concentration profiles that simultaneously optimize the fit to lidar backscatter signals and to columnar volume concentration values retrieved by the photometer. In this way the volume concentration of fine, coarse, and, possibly, coarse/non-spherical aerosol modes are retrieved.

LIRIC has proven to be a robust algorithm for aerosol volume concentration retrievals. The output of LIRIC has been validated against similar retrievals that do not rely on a specific aerosol model (Wagner et al., 2013); the comparison indicates that the spheroid model that represents non spherical particles does not induce significant errors in the retrieval. A further source of uncertainties is the choice of user-defined parameters for each retrieval; such parameters include, for example, minimum and maximum altitude, the altitude of an aerosol-free region, and regularization parameters used in the inversion. Granados-Muñoz et al. (2014) show that the retrieval is stable to the choice of these parameters; in the examples shown in that paper, the result retrieval errors remains below 20 %.

2.3 Dust models

Dust transport modeling was a point of intense research since the 1990's and several global and regional models have been developed (Tegen and Fung, 1994; Nickovic and Dobricic, 1996; Benedetti et al., 2014). In this study we focus on regional transport models setup over the domain of North Africa and Europe; these models are frequently used to predict dust transport over Europe and to explore the effects of dust in the European atmosphere.

As mentioned in the introduction, the four models used for the demonstration of the described methodology are BSC-DREAM8b v2, NMMB/BSC-Dust, DREAMABOL, and DREAM8-NMME-MACC. Being part of the SDS-WAS program, all models undergo near-real time evaluation against satellite- and ground-based columnar observations.

The Dust Regional Atmospheric Model (DREAM; Nickovic et al., 2001) is based on the Euler-type partial differential nonlinear equation for dust mass continuity and is driven by NCEP/Eta and assumes a viscous sublayer between the smooth desert surface and the lowest model layer (Janjic, 1994; Nickovic et al., 2001). The updated version of the model is the BSC-DREAM8b v2 model (Pérez et al., 2006a, b; Basart et al., 2012b) which is developed and operated at the Barcelona Supercomputing Center, Spain (BSC; http://www.bsc.es/projects/earthscience/BSC-DREAM/). It includes a set of updates including eight particle-size bins representation of the dust size distribution, improved source representation, and updated wet and dry deposition schemes. The model has been extensively evaluated against observations (e.g. Pay et al., 2010; Basart et al., 2012b, a).

The DREAMABOL model is an online integrated regional mineral dust model developed at the Institute of Atmospheric Sciences and Climate, Bologna, Italy, as part of the atmospheric composition and meteorology model BOLCHEM (Mircea et al., 2008; Maurizi et al., 2011). The meteorological component is the BOLAM primitive equation hydrostatic model (Buzzi et al., 2003). Dust model part is inspired by DREAM (Nickovic et al., 2001) but is completely rewritten and includes different assumptions on the model source and on the wet removal (Maurizi and Monti, 2015). DREAMABOL provides data to the SDS-WAS since June 2014 and participates since then in the near-real time evaluation.

AMTD
8, 3605–3666, 2015
Dust model comparison methodology
I. Binietoglou et al.

The DREAM8-NMME-MACC is developed and operated at the South East European Virtual Climate Change Center (SEEVCCC; http://www.seevccc.rs/), Serbia. The DREAM8 model is embedded in the NCEP Nonhydrostatic Mesoscale Model (NMM) on E-grid (Janjic et al., 2001) while initial and boundary conditions are taken from ECMWF global forecast. This version of DREAM8 is assimilating ECMWF dust analysis in dust initial field, with dust sources defined from Ginoux et al. (2001). DREAM8-NMME-MACC provides daily dust forecasts available at the SEEVCCC website.

Finally, the NMMB/BSC-Dust model is a regional to global dust forecast system designed and developed at BSC in collaboration with NOAA NCEP, NASA Goddard Institute for Space Studies and the International Research Institute for Climate and Society (IRI) (Pérez et al., 2011). It is an online multi-scale atmospheric dust model fully embedded into the NMM on B-grid (Janjic et al., 2011). As with DREAM, this model assumes a viscous sublayer between the smooth desert surface and the lowest model layer while it includes a physically based dust emission scheme, which explicitly takes into account saltation and sandblasting processes (White, 1979; Marticorena and Bergametti, 1995; Marticorena et al., 1997). The NMMB/BSC-Dust model has been evaluated at regional and global scales (Pérez et al., 2011; Haustein et al., 2012). It provides operational dust forecast for the Barcelona Dust Forecast Center (BDFC; http://dust.aemet.es/) the first specialized center of the WMO for dust prediction.

While each model has a different setup, they use common description of dust size distribution using 8 size bins between 0.1 and 10 µm (Pérez et al., 2011) with intervals taken from Tegen and Lacis (1996) and Pérez et al. (2006a). Dust within each transport bin is assumed to have a time-invariant log-normal distribution (Zender et al., 2003) with the shape of the distribution fixed to a mass median diameter of 2.524 µm (Shettle, 1986) and a geometric SD of 2.0 (Schulz et al., 1998). The dust mass in each bin depends on model processes. Many other subcomponents are shared between some of the models.

In the present analysis, various model output fields at 3 hourly resolution are compared. The research teams at the modeling centers configured their model experiments independently and not necessarily following the setup of their respectively daily operational forecast. The spatial resolution, domain size, initial and boundary conditions, differ, in addition to the different physical parameterizations implemented in the models summarized in Table 2.

3 Methodology

In this section we present the considerations for constructing the remote sensing dataset and choosing statistical indicators that can be used for the model and measurement cross-examination. Special attention is given in selecting a representative dataset, avoiding possible biases due to the geographical restrictions of the measurement location, the selection of vertical resolution, and the effect of local dust sources in the study of the PBL. The considerations that guided our choices are given below.

Remote sensing profiling measurements can be used to improve dust modeling efforts at three different levels: diagnostic evaluation, Near Real-Time (NRT) evaluation, and assimilation (Seigneur et al., 2000; Sicard et al., 2015; Wang et al., 2014). In the first case, remote sensing measurements are used to study the model performance during a past study period. The aim of such a study is to evaluate the model performance, understand its behavior and limitations, and suggest improvements either by tuning applied parameterizations or by changing the representation of processes in the models. The evaluation can focus on individual cases of dust transport events or follow a statistical approach, covering a larger time period.

In the case of NRT evaluation, the measured profiles are used to provide insight on the performance of an operational forecast. The aim of such an evaluation is to provide a quick overview of the model performance to the end users while it can also help modelers detect possible problems in time. The time requirements for the processing of such observations are moderately strict, as data could be useful even one day after the measurement time. In the case of assimilation, the remote sensing measurements are used by the model to improve the forecasted model concentrations. The time re-

AMTD
8, 3605–3666, 2015

quirements for assimilation depend on the assimilation system used but are typically of a few hours.

In this study we focus on the first case, that is, diagnostic evaluation of the model performance. We choose to study an extended time and space period that gives us better representation of different meteorological conditions, dust transport paths, and measurement locations. However, the considerations and metrics presented here can also be applied to the NRT evaluation scenario.

As shown in Sect. 2.2, synergistic retrieval algorithms can help avoiding possible comparison biases caused by the presence of aerosol mixtures, by separating the dust contribution from that of other aerosol types. However, direct comparison with dust models should be done carefully, because the part of aerosol identified as dust could differ depending on the selected algorithm. Thus, in the case of LIRIC dust is assumed to be a particle component larger than $\sim 0.5\,\mu m$ in radius. On the other hand, the total dust load predicted by the models also includes smaller particle sizes in the first few bins of the dust size distribution. The contribution of these small particles in the total aerosol load should be typically low, especially near the source (d'Almeida, 1987), but could become more important in cases of long-range dust transport where the larger particles have been gravitationally removed (Mamouri and Ansmann, 2014). When using a statistical approach including different locations and transport paths, as in the present study, this effect is expected to be small. The exact amount of fine-mode transported dust is an open issue and should be further investigated. The fine mode contribution, however, is expected to be important when performing a case study evaluation and then only specific bins from the model output should be used instead.

In the case of statistical model evaluation, the selected measurement profiles should also be independent to give a correct representation of the model performance. Specifically, it should be avoided that the used measurements from each station sample the same event multiple times, but should instead measure independent dust transport events. This consideration is less important when using data from automatic instruments; in the case of EARLINET, however, the available dataset could contain data

AMTD
8, 3605–3666, 2015

from long observations periods and intensive measurement campaigns, as described in Sect. 2.1. Ideally, only a climatological dataset would be used, but the number of the available cases would be limited from the measurement frequency, the sporadic nature of dust transport episodes, and, when using synergistic algorithms, the availability of AERONET data. In this study we consider to sample independent dust transport events by measurements that had at least 24 h time difference, compatible with the expected variability of tropospheric aerosols (Anderson et al., 2003a, b).

The vertical resolution of lidar and dust model profiles should be taken into account during their comparison. The lidar signals have a raw vertical resolution of a few meters and the final products have an effective resolution of a few hundred meters depending on filtering procedures and smoothness constraints used in the retrieval (Pappalardo et al., 2004). The vertical resolution of the models, on the other hand, is typically coarser but depends on the vertical resolution of the meteorological driver (Simmons and Burridge, 1981; Mesinger, 1984). When performing a statistical comparison, the different vertical resolutions are less important as the features of individual dust transport cases will be smoothed. When comparing aerosol extensive properties (both optical and concentrations) the remote sensing profiles should be upscaled to the model resolution. When, however, the aim of the comparison is to evaluate the dust layer geometrical properties and values at a specific location, e.g. the peak concentration values, the finer resolution remote sensing profiles should be used. In this study and in order to facilitate the comparison of models of different vertical resolutions, we interpolate all available profiles to a common 100 m vertical resolution. We used this resolution to examine the geometrical properties and peak concentration value of dust layers, but used 500 m averages to calculate the statistics on the vertical profiles presented in the next section. The models simulate the dust concentration profiles on a specified horizontal grid, so bilinear interpolation was used to estimate the concentration values at the exact location for each station. Linear interpolation was also utilized to estimate the concentration profiles at the exact time of the available measurements.

AMTD
8, 3605–3666, 2015

Correct representation of the dust mixing in the PBL can impact the forecasted air quality and also affect the removal processes of dust in the model. In this process, dust is mixed with locally produced aerosols, so lidar optical profiles cannot be used to directly study the dust effect. The mass retrieval algorithms, like LIRIC, are able to separate the dust component in the PBL and give some insights to study this process, even though several limitations remain. Firstly, local dust sources could contribute to the dust load in the PBL (Korcz et al., 2009) although the exact effect of such sources to the vertical dust distribution, to our knowledge, has not been systematically studied. Secondly, as dust comes in contact with other types of particles and high relative humidity, some of the assumptions of the retrieval algorithms could be invalid. For example, polluted and humid PBL can lead to dust being coated and water layer to form on the dust particles, changing their optical properties (Levin et al., 1996; Kumar et al., 2011b). Such effect could be important for the exact quantitative characterization of dust but does not completely prevent studying the mixing of dust in the PBL. Lastly, most lidar systems have a high overlap function and can only detect the initial mixing of dust in the upper parts of the PBL. Given these factors, the study of this mixing process could be done better for specific case studies. If a statistical approach is followed, the dataset should be large enough to give significant results, as only few profiles cannot capture this dynamical mixing phenomenon.

The direct output of all the synergistic retrieval algorithm mentioned before is volume concentration profiles of fixed aerosol types. This can be converted to mass concentration profiles, the typical output of dust transport models, by using the aerosol bulk density. In the case of dust, the typically used value is $2.6\,\mathrm{g\,cm^{-3}}$ (Köpke et al., 1997; Ansmann et al., 2012) while the actual bulk concentration could differ by location (e.g. Todd et al., 2007). In the case of dust model evaluation, however, selecting a value of $2.6\,\mathrm{g\,cm^{-3}}$ is compatible with the assumptions of most dust transport models (Tegen and Fung, 1994; Nickovic et al., 2001; Yumimoto et al., 2012), and thus a further reason for discrepancies is removed from this study.

AMTD
8, 3605–3666, 2015

We perform the comparison firstly by examining single statistical indicators of each measurement case and secondly looking into indicators at different altitude ranges. This approach allows assessing both the total performance of the models and the detailed performance across the profile. The single parameters examined are total concentration, peak concentration value, and center of mass of the dust vertical distribution. For the profile parameters, apart from the average profiles, we examine the mean bias error, correlation coefficient, root mean square error, and fractional gross error. This set of parameters was chosen because it can provide a detailed view of performance while remaining compatible, as much as possible, with the metrics already in use in the SDS-WAS columnar evaluation.

An important indicator for model vertical profiles is the center of mass (CoM), a parameter that gives in a single number an indication of the altitude of the dust distribution. In cases were a single aerosol layer is present in the atmosphere, the CoM gives an indication of its mean altitude; in case of multiple layers, however, the CoM could be located in areas without any considerable dust load (Mona et al., 2006, 2014).

The second single-value measure to compare is the dust total concentration, calculated across the altitude range where both measured and model profiles provide valid results. In this way, this comparison will be a little different than comparing directly columnar measurements, as in the case of comparing photometer and total column model values. In the latter case the used range includes the lower few hundred meters of the profile, thus including the contribution of local dust sources to the total column aerosol load, possibly producing a bias in the measurements.

A third metric examined is the peak value of the profile, a value typically indicating the main vertical location of the dust plume. In cases where the main dust mass is located near the ground, the lidar system can fail to detect the true maximum, and instead show a maximum value at the lowest point of the profile, i.e. first point of full overlap. In these cases we considered as maximum value the first lofted layer peak, located as the first peak after the first local minimum of the concentration profile.

AMTD
8, 3605–3666, 2015

The profile statistical indicators were calculated by first averaging the compared profiles at 500 m resolution then computing a set of statistics for each altitude range. This resolution was chosen as a trade-off between detailed aerosol structure and the signal noise of the lidar measurements. This value, however, needs to be determined in each study based on the number of available profiles. Apart from the mean value profiles, the first set of metrics used are the mean bias, and the root mean square error (RMSE); being expressed in units of concentration, these values are suitable for the intercomparison of models but can be misleading for the performance of models with altitude. In addition, RMSE is strongly dominated by the largest values, due to the squaring operation, so in cases where prominent outliers occur, the usefulness of RMSE is questionable and the interpretation becomes more difficult. These limitations are addressed using a second set of statistical indicators, including correlation coefficient, fractional bias, and fractional gross error. Fractional bias is a normalized measure of the mean bias and indicates only systematic errors which lead to under/over-estimation of the measured values. Similarly, the fractional gross error is a positive-defined indicator that gives the same figure with respect to under- and over-estimation. Definitions of the used statistical indicators are given in Table 3.

4 Results and discussion

In this section we apply the described methodology to simulations performed by the four models described in Sect. 2.3. Ten European remote sensing stations contributed data to this intercomparison, mainly concentrated in the Mediterranean area, as shown in Fig. 1. Their location and data supplied can be seen in Table 4. All stations are part of the EARLINET and AERONET networks, a fact that guarantees that the provided data are of uniform quality. The participating stations provided, in total, 61 LIRIC retrievals of dust profiles for an agreed time period of January 2011 to February 2013. The time difference between lidar and photometer measurements was kept as small as possible (72 % – < 1 h, 93 % – < 3 h). In all cases attention was given to have stable

AMTD
8, 3605–3666, 2015

atmospheric conditions between the measurements of the two instruments. The majority of cases is located in spring and summer period (see Fig. 2), when most Saharan dust transport episodes occur over Europe and cloud-free conditions, needed for the measurements, are usually found (Mona et al., 2006; Papayannis et al., 2008). The stations selected the cases independently, based on the available measurements. For each station, the selected profiles were screened for having at least 24 h time distance, as described before, to consider only measurements of different dust transport events. The actual number of available measurements varies with altitude as shown in Fig. 3. In the lower altitudes, the number is limited by the ground level altitude of the stations and the incomplete measurement range of the instruments. In the higher altitude the lidar profiles were cut at the points were no dust was further detected. The four examined dust transport models were run for the given period and the output was stored for three hour intervals.

The comparison based on center of mass (CoM) reveals that models do correctly track the main vertical location of transport dust. In Fig. 4 this comparison is presented for the four models, and shows that the models perform well in forecasting the dust CoM in almost all cases. The difference of predicted and measured CoM exceeds 1 km only in 4 cases (7 %) for BSC-DREAM8b v2 and DREAMABOL in 10 cases (16 %) for NMMB/BSC-DUST and 8 cases (13 %) for DREAM8-NMME-MACC. The BSC-DREAM8b v2 and DREAMABOL models show almost zero bias tracking the location of dust almost perfectly, except in few outlying cases. These are cases where the model practically does not predict the transport even, and the CoM is determined by some residual concentration in the profile. Instead, NMMB/BSC-DUST and DREAM8-NMME-MACC overestimate the center of mass altitude, especially in cases with observed CoM above 3 km; the fractional bias values for NMMB/BSC-DUST and DREAM8-NMME-MACC are 0.16 and 0.13 respectively. The correlation coefficient, especially for BSC-DREAM8b v2, is determined by the few extreme cases; the values for the four models are 0.60 for BSC-DREAM8b v2, 0.72 for DREAMABOL, and 0.79 for NMMB/BSC-DUST and DREAM8-NMME-MACC.

Our examination indicates that the simulations systematically underestimate the total amount of dust. Figure 5 presents the comparison of the dust concentration integrated across the common altitude range for each case. The volume concentration from the four models shows significant correlation with the measured one, but in general is underestimated. For high concentration cases (values greater than $\sim 0.3\,\mathrm{g\,m^{-2}}$) NMMB/BSC-DUST and DREAM8-NMME-MACC predict sufficiently well the concentration values, while the other two models tend to underestimate. For low concentration values (less than $0.3\,\mathrm{g\,m^{-2}}$) all models apart from DREAM8-NMME-MACC underestimate in many cases the dust concentration. This could be caused by insufficient dust source strength, overestimated deposition and wet scavenging parameters, or a combination of both; the current dataset is not sufficient to discriminate the exact factor affecting the comparison from the model point of view. It is believed, however, that using the present approach as part of a complete, multi-sensor evaluation exercise would help investigating possible model limitations. The improved performance of DREAM8-NMME-MACC could be attributed to the assimilation scheme used only by this model. The total fractional bias values for the models range from −1.05 to −0.25, while correlation coefficients range from 0.52 to 0.82.

Figure 6 shows the relationship of peak simulated values for each profile and the measured ones. Also in this case, the models underestimate the maximum value of each profile. The fractional bias for the four models ranges from −0.89 to −0.31 while the correlation coefficient has smaller values than before from 0.52 to 0.72. This result can only partly be explained by the overall concentration underestimation that was noted before. The lower original resolution of the models, compared to the lidar, could lead to a "smoothing" effect of individual peak values in the compared cases. A similar effect could be caused by the mixing of the dust in all the volume of the model's grid. A summary of the above described statistics for all the examined models is given in Table 5.

In summary, the current study indicates that the examined dust models represent well the altitude of transport while the total concentration is predicted lower than mea-

AMTD
8, 3605–3666, 2015

sured, with sharp peaks smoothed out. The performance of models in specific cases, however, can vary significantly. Figure 7 summarizes the performance of all models on a case-by-case comparison. For each model-measurement pair we calculate the vertical correlation coefficient of the volume concentration profiles as well as the fractional bias, and the results are plotted in a scatterplot. The ideal model would have correlation one, i.e. it would predict perfectly the shape of the dust profile, and 0 fractional bias, i.e. predicting correctly the quantity of transported dust. While individual cases show a big variability, each model shows a characteristic pattern. For BSC-DREAM8b v2 and DREAMABOL most cases have high correlation but negative fractional bias i.e. the models can often predict correctly the shape of the dust profile but underestimate the concentration. In contrast, NMMB/BSC-DUST and DREAM8-NMME-MACC have fractional bias value distribution near 0 but a wider spread of correlation values. For all models, it should be observed that there is a considerable spread of values for the specific comparisons, a further argument for the need for a statistical evaluation of dust model performance.

These results are further supported by directly comparing the profile data provided by the model, indicating that models do not only capture the general altitude of dust transport but, on average, predict correctly the shape of the dust profile. In Fig. 8 the mean measured concentration profile for all 61 cases is compared with the corresponding profiles of the four models. The profiles show good agreement in the predicted shape of the dust concentration, but have wider spread in the absolute values. BSC-DREAM8b v2 and DREAMABOL predict the maximum dust concentration in the region 2–3 km a.s.l., in agreement with the observations, while the other two models have the maximum value at slightly higher altitude of 3–4 km. DREAM8-NMME-MACC overestimates the concentration of dust in altitudes above ~ 5 km; specifically, while the observed values of dust are below 10 $\mu g\,m^{-3}$ above 6 km, the model predicts these values only above 8 km. The concentration values show wider discrepancy: while the peak value of the mean profiles is retrieved at ~ 65 $\mu g\,m^{-3}$ the models peak values range from ~ 30 to ~ 50 $\mu g\,m^{-3}$. The observed increased concentration at high alti-

AMTD
8, 3605–3666, 2015

tudes in some models could be related to misrepresentation of the tropopause (Janjic, 1994; Mona et al., 2014) that normally limits the maximum altitude of dust transport. In higher altitudes, the main removal mechanism of dust is sedimentation, and the removal of any dust reaching high altitudes is slower, allowing the artificial accumulation of dust. When examining the profile data, we can observe the differences in high and low concentration cases that were described before, as shown in Fig. 9. NMMB/BSC-DUST and DREAM8-NMME-MACC have particularly good agreement at the high concentration cases. As noted before, such findings highlight the importance of statistical comparison approach and indicate that this trend should be investigated in a future complete evaluation study.

The above results are further explored in Figs. 10–13. Figure 10 presents the mean bias of the four studied models. All models show negative bias below 4 km while above that altitude NMMB/BSC-DUST has almost 0 bias and DREAM8-NMME-MACC has positive bias values. At the altitude range where most dust is located, i.e. from 2 to 4 km a.s.l., the maximum biases range from −40 to 0 $\mu g\,m^{-3}$. In Fig. 11 the variation of the RMSE with altitude is shown. In the 2–4 km range the mean values range from 40 to 67 $\mu g\,m^{-3}$ with the maximum value reached by DREAMABOL at 2 km a.s.l. The profiles of correlation coefficient for the four models are shown in Fig. 12. All four models show significant correlation for altitude range from 1 to 6 km, which is the region where most dust particles are typically observed (Mona et al., 2006). The mean values range from 0.50 for DREAMABOL to 0.65 for DREAM8-NMME-MACC. Finally, in Fig. 13 the fractional gross error is shown. The minimum values for F_E, ranging from 0.77 to 1.14, are observed at 2–4 km. At higher altitudes, the F_E values are higher, with values ranging from 1.28 to 1.66 at 6 km a.s.l.

A summary of the different behavior of the four models is given in Fig. 14 using Taylor diagrams (Taylor, 2001). The data of the models and measurements were averaged at 1 km altitude ranges before calculating the statistics, to give an overview of the model performance at these regions. Four Taylor diagrams are presented, for the altitude range from 1 to 5 km. DREAM8-NMME-MACC seems to capture correctly the range of

AMTD
8, 3605–3666, 2015

values of the dust events in all altitude ranges, a property that can partly be attributed to the use of data assimilation. NMMB/BSC-DUST shows similar good performance, especially for 3 to 5 km. As observed before, the other two models underestimate the variability of dust in a consistent way with altitude. The model simulations have correlations from 0.4 to 0.8 at all four altitude ranges.

The presented results depend on regional and seasonal variations. While the available cases in this study are not sufficient to perform a seasonal analysis, they can be used to get a hint of the insight that can be gained from a regional evaluation of the model performance. With this aim, the available stations were divided in two clusters, a west and an east one. The west cluster of stations, including Evora, Granada, and Barcelona, is affected by dust events arriving only after a few days of transport. The east cluster, including Potenza, Lecce, Athens, Thessaloniki, and Bucharest, is affected by longer transport of dust from both the West and Central Sahara. The regional comparison of the mean dust concentration profiles is shown in Fig. 15. The average profiles indicate that the dust is transported at different altitudes, with the maximum value observed around 2 km a.s.l. for the west cluster and around 3 km a.s.l. for the east cluster, a behavior that is well captured by all models. The correlation coefficient at all altitudes is higher for the east rather than the west cluster as shown in Fig. 16. Specifically, the average correlation at the altitude range from 2 to 5 km ranges for the west cluster from 0.50 to 0.70 and for the east cluster from 0.55 to 0.87. This difference can be attributed to the strong effect of orography on the west cluster, as Atlas Mountains and orography of the Iberian Peninsula make the prediction of the dust transport difficult, while the transport to the East cluster is performed, for large part of the transport path, over the Mediterranean Sea. Additionally, the longer transport to the east cluster, typically 1–2 days longer according to back-trajectory analysis, homogenizes the dust transport event and makes small inconsistencies in space and time less relevant. These preliminary results indicate that the regional aspects in prediction of the vertical distribution of dust should be further studied.

AMTD
8, 3605–3666, 2015

5 Conclusions

A methodology for the examination of dust model data using volume concentration profiles retrieved using the synergy of lidar and sun photometer has been presented. The proposed approach adapts previous experience from SDS-WAS to the use of dust volume concentration profiles. The methodology was applied for the examination of 4 dust models using 61 dust concentration profiles retrieved from EARLINET/AERONET station across Europe using the LIRIC algorithm.

This first comparison presented is a clear indication that the representation of dust vertical structure by dust models needs to be further explored. The four models can individually predict different aspects of dust transport, but show considerable differences in their performance despite many similarities in their setup, including the number of dust size bins and deposition processes. The reasons for these differences should be the topic of future evaluation studies including a variety of sensors, e.g. AERONET photometer and satellite AOD measurements, to explore different aspects of dust modeling systems. This is a further indication that ensemble dust models products should be considered to improve the forecast quality.

Additionally, the results presented provide indications for future developments needed in the observational infrastructure and remote sensing algorithms used. The number of available remote sensing measurement should increased to allow better characterization of regional and seasonal aspects of model performance. For this to happen, automatic retrieval algorithms and continuous operating lidar systems should be developed and used. This would also allow the near-real time evaluation of dust models, providing important feedback both to modelers and end-user communities. A further step needed from the retrieval algorithms perspective is a better characterization of the error, both at statistical and systematic level. This will allow distinguishing more subtle effect in different model setups. Such improvements are actively pursued in the framework of ACTRIS and other projects across Europe.

AMTD
8, 3605–3666, 2015

In total we believe that this study is an important step toward the systematic use of remote sensing atmospheric profiling measurements to model-evaluation studies. The increase availability of advanced profiling data from multi wavelength lidars and sun photometers will form a solid base to improve dust model performance and lead to better understanding of the effect of dust on air-quality, weather and the climate.

Acknowledgements. The financial support of the ACTRIS Research Infrastructure Project supported by the European Union Seventh Framework Programme (FP7/2007-2013) under grant agreement no. 262254 is gratefully acknowledged. This project has also received funding from the European Union's Seventh Framework Programme for research, technological development and demonstration under grant agreement no. 289923 – ITaRS. S. Basart and J. M. Baldasano acknowledge the CICYT project (CGL2010-19652 and CGL2013-46736) and Severo Ochoa (SEV-2011-00067) programme of the Spanish Government. This program has received funding from the Ministry of Education and Science of the Republic of Serbia through project III43007. BSC-DREAM8b and NMMB/BSC-Dust simulations were performed on the Mare Nostrum supercomputer hosted by Barcelona Supercomputing Center-Centro Nacional de Supercomputación (BSC-CNS). We thank the AERONET PI's and their staff for establishing and maintaining the 10 sites used in this investigation. The authors would like to acknowledge the use of Google maps for the images used for realizing Fig. 1. We would also like to thank Slobodan Nickovic for his support and comments during the preparation of this manuscript.

References

Althausen, D., Engelmann, R., Baars, H., Heese, B., Ansmann, A., Müller, D., and Komppula, M.: Portable Raman Lidar PollyXT for automated profiling of aerosol backscatter, extinction, and depolarization, J. Atmos. Ocean. Tech., 26, 2366–2378, doi:10.1175/2009JTECHA1304.1, 2009. 3649

Anderson, T. L., Charlson, R. J., Winker, D. M., Ogren, J. A., and Holmén, K.: Mesoscale variations of tropospheric aerosols, J. Atmos. Sci., 60, 119–136, 2003a. 3621

Anderson, T. L., Masonis, S. J., Covert, D. S., Ahlquist, N. C., Howell, S. G., Clarke, A. D., and McNaughton, C. S.: Variability of aerosol optical properties derived from in situ aircraft measurements during ACE-Asia, J. Geophys. Res., 108, 8647, doi:10.1029/2002JD003247, 2003b. 3621

Ansmann, A., Riebesell, M., Wandinger, U., Weitkamp, C., Voss, E., Lahmann, W., and Michaelis, W.: Combined Raman elastic-backscatter lidar for vertical profiling of moisture, aerosol extinction, backscatter, and lidar ratio, Appl. Phys. B, 55, 18–28, 1992. 3613

Ansmann, A., Tesche, M., Seifert, P., Groß, S., Freudenthaler, V., Apituley, A., Wilson, K. M., Serikov, I., Linné, H., Heinold, B., Hiebsch, A., Schnell, F., Schmidt, J., Mattis, I., Wandinger, U., and Wiegner, M.: Ash and fine-mode particle mass profiles from EARLINET-AERONET observations over central Europe after the eruptions of the Eyjafjallajökull volcano in 2010, J. Geophys. Res., 116, D00U02, doi:10.1029/2010JD015567, 2011. 3615

Ansmann, A., Seifert, P., Tesche, M., and Wandinger, U.: Profiling of fine and coarse particle mass: case studies of Saharan dust and Eyjafjallajökull/Grimsvötn volcanic plumes, Atmos. Chem. Phys., 12, 9399–9415, doi:10.5194/acp-12-9399-2012, 2012. 3610, 3615, 3622

Balkanski, Y., Schulz, M., Claquin, T., and Guibert, S.: Reevaluation of Mineral aerosol radiative forcings suggests a better agreement with satellite and AERONET data, Atmos. Chem. Phys., 7, 81–95, doi:10.5194/acp-7-81-2007, 2007. 3608

Barbosa, H. M. J., Lopes, F. J. S., Silva, A., Nisperuza, D., Barja, B., Ristori, P., Gouveia, D. A., Jimenez, C., Montilla, E., Mariano, G. L., Landulfo, E., Bastidas, A., and Quel, E. J.: The first ALINE measurements and intercomparison exercise on lidar inversion algorithms, Optica pura y aplicada, 47, 99–108, 2014. 3611

Basart, S., Pérez, C., Cuevas, E., Baldasano, J. M., and Gobbi, G. P.: Aerosol characterization in Northern Africa, Northeastern Atlantic, Mediterranean Basin and Middle East from direct-sun AERONET observations, Atmos. Chem. Phys., 9, 8265–8282, doi:10.5194/acp-9-8265-2009, 2009. 3609

Basart, S., Pay, M. T., Jorba, O., Pérez, C., Jiménez-Guerrero, P., Schulz, M., and Baldasano, J. M.: Aerosols in the CALIOPE air quality modelling system: evaluation and analysis of PM levels, optical depths and chemical composition over Europe, Atmos. Chem. Phys., 12, 3363–3392, doi:10.5194/acp-12-3363-2012, 2012a. 3617

Basart, S., Pérez, C., Nickovic, S., Cuevas, E., and Baldasano, J. M.: Development and evaluation of the BSC-DREAM8b dust regional model over Northern Africa, the Mediterranean and the Middle East, Tellus B, 64, 18539, doi:10.3402/tellusb.v64i0.18539, 2012b. 3609, 3617

Benedetti, A., Morcrette, J.-J., Boucher, O., Dethof, A., Engelen, R. J., Fisher, M., Flentje, H., Huneeus, N., Jones, L., Kaiser, J. W., Kinne, S., Mangold, A., Razinger, M., Simmons, A. J.,

AMTD
8, 3605–3666, 2015

Dust model comparison methodology

I. Binietoglou et al.

and Suttie, M.: Aerosol analysis and forecast in the European centre for medium-range weather forecasts integrated forecast system: 2. Data assimilation, J. Geophys. Res., 114, D13205, doi:10.1029/2008JD011115, 2009. 3609
Benedetti, A., Baldasano, J. M., Basart, S., Benincasa, F., Boucher, O., Brooks, M. E., Chen, J.-P., Colarco, P. R., Gong, S., Huneeus, N., Jones, L., Lu, S., Menut, L., Morcrette, J.-J., Mulcahy, J., Nickovic, S., García-Pando, C. P., Reid, J. S., Sekiyama, T. T., Tanaka, T. Y., Terradellas, E., Westphal, D. L., Zhang, X.-Y., and Zhou, C.-H.: Operational dust prediction, in: Mineral Dust, edited by: Knippertz, P. and Stuut, J.-B. W., Springer, Dordrecht, Netherlands, 223–265, 2014. 3617, 3647
Betts, A. K.: A new convective adjustment scheme. Part I: Observational and theoretical basis, Q. J. Roy. Meteor. Soc., 112, 677–691, doi:10.1002/qj.49711247307, 1986. 3647
Buzzi, A., D'Isidoro, M., and Davolio, S.: A case-study of an orographic cyclone south of the Alps during the MAP SOP, Q. J. Roy. Meteor. Soc., 129, 1795–1818, doi:10.1256/qj.02.112, 2003. 3617
Böckmann, C., Wandinger, U., Ansmann, A., Bösenberg, J., Amiridis, V., Boselli, A., Delaval, A., De Tomasi, F., Frioud, M., Grigorov, I. V., Hågård, A., Horvat, M., Iarlori, M., Komguem, L., Kreipl, S., Larchevêque, G., Matthias, V., Papayannis, A., Pappalardo, G., Rocadenbosch, F., Rodrigues, J. A., Schneider, J., Shcherbakov, V., and Wiegner, M.: Aerosol lidar intercomparison in the framework of the EARLINET project. 2. Aerosol backscatter algorithms, Appl. Optics, 43, 977–989, 2004. 3612
Bösenberg, J., Ansmann, A., Baldasano, J. M., Calpini, B., Chaikovsky, A., Flamant, P., Mitev, V., Flamant, A., Hågård, A., Mitev, V., Papayannis, A., Pelon, J., Resendes, D., Schneider, J., Spinelli, N., Trickl, T., Vaughan, G., Visconti, G., and Wiegner, M.: EARLINET: a European aerosol research lidar network, in: Advances in Laser Remote Sensing, edited by: Dabas, A., Loth, C., and Pelon, J., 155–158, Ecole Polytechnique, Palaiseau Cedex, France, 2001. 3611
Campbell, J. R., Hlavka, D. L., Welton, E. J., Flynn, C. J., Turner, D. D., Spinhirne, J. D., Scott, V. S., and Hwang, I. H.: Full-time, eye-safe cloud and aerosol lidar observation at atmospheric radiation measurement program sites: instruments and data processing, J. Atmos. Ocean. Tech., 19, 431–442, 2002. 3611
Chaikovsky, A., Dubovik, O., Goloub, P., Tanré, D., Pappalardo, G., Wandinger, U., Chaikovskaja, L., Denisov, S., Grudo, Y., Lopatsin, A., Karol, Y., Lapyonok, T., Korol, M., Osipenko, F., Savitski, D., Slesar, A., Apituley, A., Alados-Arboledas, L., Binietoglou, I., Kokkalis, P., Munoz, M. J. G., Papayannis, A., Perrone, M. R., Pietruczuk, A., Pisani, G.,

AMTD
8, 3605–3666, 2015

Dust model comparison methodology

I. Binietoglou et al.

Rocadenbosch, F., Sicard, M., De Tomasi, F., and Wang, X.: Algorithm and software for the retrieval of vertical aerosol properties using combined lidar/radiometer data: dissemination in EARLINET, Proceedings, 26th International Laser Radar Conference, Porto Heli, Greece, 399–402, 2012. 3610, 3615

Chaikovsky, A., Dubovik, O., Goloub, P., Holben, B., Tanre, D., Pappalardo, G., Wandinger, U., Chaikovskaya, L., Denisov, S., Grudo, Y., Lopatin, A., Amiridis, V., Ansmann, A., Apituley, A., Arboledas, L. A., Binietoglou, I., Freudenthaler, V., Kokkalis, P., Granados-Muñoz, M. J., Nicolae, D., Papayannis, A., Perrone, M. R., Pietruczuk, A., Pisani, G., Rocadenbosch, F., Sicard, M., Talianu, C., Tsekeri, A., De Tomasi, F., Wagner, J., and Wang, X.: Lidar-Radiometer Inversion Code (LIRIC) for the retrieval of vertical aerosol properties using combined lidar/radiometer data: development and distribution in EARLINET, Atmos. Meas. Tech. Discuss., in preparation, 2015. 3610, 3615

Cuesta, J., Flamant, P. H., and Flamant, C.: Synergetic technique combining elastic backscatter lidar data and sunphotometer AERONET inversion for retrieval by layer of aerosol optical and microphysical properties, Appl. Optics, 47, 4598–4611, doi:10.1364/AO.47.004598, 2008. 3615

Cuevas, E., Camino, C., Benedetti, A., Basart, S., Terradellas, E., Baldasano, J. M., Morcrette, J.-J., Marticorena, B., Goloub, P., Mortier, A., Berjón, A., Hernández, Y., Gil-Ojeda, M., and Schulz, M.: The MACC-II 2007–2008 reanalysis: atmospheric dust evaluation and characterization over Northern Africa and Middle East, Atmos. Chem. Phys. Discuss., 14, 27797–27879, doi:10.5194/acpd-14-27797-2014, 2014. 3609

d'Almeida, G. A.: On the variability of desert aerosol radiative characteristics, J. Geophys. Res., 92, 3017–3026, doi:10.1029/JD092iD03p03017, 1987. 3620

DeMott, P. J., Sassen, K., Poellot, M. R., Baumgardner, D., Rogers, D. C., Brooks, S. D., Prenni, A. J., and Kreidenweis, S. M.: African dust aerosols as atmospheric ice nuclei, Geophys. Res. Lett., 30, 1732, doi:10.1029/2003GL017410, 2003. 3608

Dubovik, O.: Optimization of numerical inversion in photopolarimetric remote sensing, in: Photopolarimetry in Remote Sensing, edited by: Videen, G., Yatskiv, Y., and Mishchenko, M., no. 161 in NATO Science Series II: Mathematics, Physics and Chemistry, Springer, Dordrecht, Netherlands, 65–106, 2005. 3615

Dubovik, O. and King, M. D.: A flexible inversion algorithm for retrieval of aerosol optical properties from Sun and sky radiance measurements, J. Geophys. Res., 105, 673–20, 2000. 3613

AMTD
8, 3605–3666, 2015

Dubovik, O., Sinyuk, A., Lapyonok, T., Holben, B. N., Mishchenko, M., Yang, P., Eck, T. F., Volten, H., Muñoz, O., Veihelmann, B., van der Zande, W. J., Leon, J.-F., Sorokin, M., and Slutsker, I.: Application of spheroid models to account for aerosol particle nonsphericity in remote sensing of desert dust, J. Geophys. Res., 111, D11208, doi:10.1029/2005JD006619, 2006. 3613

Ferrier, B. S., Jin, Y., Lin, Y., Black, T., Rogers, E., and DiMego, G.: Implementation of a new grid-scale cloud and precipitation scheme in the NCEP Eta model, in: Proceedings of the 15th Conf. on Numerical Weather Prediction, vol. 19, Am. Meteor. Soc., San Antonio, TX, USA, 12–16 August 2002, 280–283, 2002. 3647

Gallisai, R., Peters, F., Volpe, G., Basart, S., and Baldasano, J. M.: Saharan dust deposition may affect phytoplankton growth in the Mediterranean sea at ecological time scales, PLoS ONE, 9, e110762, doi:10.1371/journal.pone.0110762, 2014. 3608

Ginoux, P., Chin, M., Tegen, I., Prospero, J. M., Holben, B., Dubovik, O., and Lin, S.-J.: Sources and distributions of dust aerosols simulated with the GOCART model, J. Geophys. Res.-Atmos., 106, 20255–20273, doi:10.1029/2000JD000053, 2001. 3618, 3647

Gobbi, G. P., Angelini, F., Barnaba, F., Costabile, F., Baldasano, J. M., Basart, S., Sozzi, R., and Bolignano, A.: Changes in particulate matter physical properties during Saharan advections over Rome (Italy): a four-year study, 2001–2004, Atmos. Chem. Phys., 13, 7395–7404, doi:10.5194/acp-13-7395-2013, 2013. 3609

Granados-Muñoz, M. J., Guerrero-Rascado, J. L., Bravo-Aranda, J. A., Navas-Guzmán, F., Valenzuela, A., Lyamani, H., Chaikovsky, A., Wandinger, U., Ansmann, A., Dubovik, O., Grudo, J. O., and Alados-Arboledas, L.: Retrieving aerosol microphysical properties by Lidar-Radiometer Inversion Code (LIRIC) for different aerosol types, J. Geophys. Res.-Atmos., 119, 4836–4858, 2014. 3616

Guerrero-Rascado, J. L., Olmo, F. J., Avilés-Rodríguez, I., Navas-Guzmán, F., Pérez-Ramírez, D., Lyamani, H., and Alados Arboledas, L.: Extreme Saharan dust event over the southern Iberian Peninsula in september 2007: active and passive remote sensing from surface and satellite, Atmos. Chem. Phys., 9, 8453–8469, doi:10.5194/acp-9-8453-2009, 2009. 3649

Guerrero-Rascado, J. L., Landulfo, E., Antuña, J. C., Barbosa, H. M. J., Barja, B., Bastidas, A. E., Bedoya, A. E., da Costa, R., Estevan, R., Forno, R. N., Gouveia, D. A., Jiménez, C., Larroza, E. G., Lopes, F. J. S., Montilla-Rosero, E., Moreira, G. A., Nakaema, W. M., Nisperuza, D., Otero, L., Pallotta, J. V., Papandrea, S., Pawelko, E.,

AMTD
8, 3605–3666, 2015

Dust model comparison methodology

I. Binietoglou et al.

Quel, E. J., Ristori, P., Rodrigues, P. F., Salvador, J., Sánchez, M. F., and Silva, A.: Towards an instrumental harmonization in the framework of LALINET: dataset of technical specifications, Proc. SPIE, 9246, 92460O–92460O-14, doi:10.1117/12.2066873, 2014. 3611

Haustein, K., Pérez, C., Baldasano, J. M., Jorba, O., Basart, S., Miller, R. L., Janjic, Z., Black, T., Nickovic, S., Todd, M. C., Washington, R., Müller, D., Tesche, M., Weinzierl, B., Esselborn, M., and Schladitz, A.: Atmospheric dust modeling from meso to global scales with the online NMMB/BSC-Dust model – Part 2: Experimental campaigns in Northern Africa, Atmos. Chem. Phys., 12, 2933–2958, doi:10.5194/acp-12-2933-2012, 2012. 3618

Heinold, B., Tegen, I., Esselborn, M., Kandler, K., Knippertz, P., Müller, D., Schladitz, A., Tesche, M., Weinzierl, B., Ansmann, A., Althausen, D., Laurent, B., Massling, A., Müller, T., Petzold, A., Schepanski, K., and Wiedensohler, A.: Regional Saharan dust modelling during the SAMUM 2006 campaign, Tellus B, 61, 307–324, doi:10.1111/j.1600-0889.2008.00387.x, 2009. 3609

Hess, M., Koepke, P., and Schult, I.: Optical properties of aerosols and clouds: The software package OPAC, B. Am. Meteorol. Soc., 79, 831–844, 1998. 3615

Holben, B. N., Eck, T. F., Slutsker, I., Tanre, D., Buis, J. P., Setzer, A., Vermote, E., Reagan, J. A., Kaufman, Y. J., and Nakajima, T.: AERONET a federated instrument network and data archive for aerosol characterization, Remote Sens. Environ, 66, 1–16, 1998. 3612

Janjic, Z., Janjic, T., and Vasic, R.: A class of conservative fourth-order advection schemes and impact of enhanced formal accuracy on extended-range forecasts, Mon. Weather Rev., 139, 1556–1568, doi:10.1175/2010MWR3448.1, 2011. 3618

Janjic, Z. I.: The step-mountain eta coordinate model: further developments of the convection, viscous sublayer, and turbulence closure schemes, Mon. Weather Rev., 122, 927–945, 1994. 3617, 3628, 3647

Janjic, Z. I., Gerrity, J. P., and Nickovic, S.: An alternative approach to nonhydrostatic modeling, Mon. Weather Rev., 129, 1164–1178, 2001. 3618

Jiménez-Guerrero, P., Pérez, C., Jorba, O., and Baldasano, J. M.: Contribution of Saharan dust in an integrated air quality system and its on-line assessment, Geophys. Res. Lett., 35, L03814, doi:10.1029/2007GL031580, 2008. 3608

Karydis, V. A., Kumar, P., Barahona, D., Sokolik, I. N., and Nenes, A.: On the effect of dust particles on global cloud condensation nuclei and cloud droplet number, J. Geophys. Res., 116, D23204, doi:10.1029/2011JD016283, 2011. 3608

Kim, S.-W., Yoon, S.-C., Dutton, E. G., Kim, J., Wehrli, C., and Holben, B. N.: Global surface-based sun photometer network for long-term observations of column aerosol optical properties: intercomparison of aerosol optical depth, Aerosol Sci. Tech., 42, 1–9, doi:10.1080/02786820701699743, 2008. 3612
Klein, H., Nickovic, S., Haunold, W., Bundke, U., Nillius, B., Ebert, M., Weinbruch, S., Schuetz, L., Levin, Z., Barrie, L. A., and Bingemer, H.: Saharan dust and ice nuclei over Central Europe, Atmos. Chem. Phys., 10, 10211–10221, doi:10.5194/acp-10-10211-2010, 2010. 3608
Klett, J. D.: Stable analytical inversion solution for processing lidar returns, Appl. Optics, 20, 211–220, 1981. 3613
Klett, J. D.: Lidar inversion with variable backscatter/extinction ratios, Appl. Optics, 24, 1638–1643, doi:10.1364/AO.24.001638, 1985. 3613
Kokkalis, P., Papayannis, A., Mamouri, E, R., Tsaknakis, G., and Amiridis, V.: The EOLE lidar system of the National Technical University of Athens, Proceedings, 26th International Laser Radar Conference, Porto Heli, Greece, 629–632, 2012 3649
Korcz, M., Fudala, J., and Kliś, C.: Estimation of wind blown dust emissions in Europe and its vicinity, Atmos. Environ., 43, 1410–1420, doi:10.1016/j.atmosenv.2008.05.027, 2009. 3622
Kovalev, V. A. and Eichinger, W. E.: Elastic Lidar: Theory, Practice, and Analysis Methods, John Wiley and Sons, New York, USA, 2004. 3613
Kumar, D., Rocadenbosch, F., Sicard, M., Comeron, A., Muñoz, C., Lange, D., Tomás, S., and Gregorio, E.: Six-channel polychromator design and implementation for the UPC elastic/Raman LIDAR, in: SPIE Remote Sensing, International Society for Optics and Photonics, Prague, Czech Republic, 81820W–81820W, 2011a. 3649
Kumar, P., Sokolik, I. N., and Nenes, A.: Measurements of cloud condensation nuclei activity and droplet activation kinetics of fresh unprocessed regional dust samples and minerals, Atmos. Chem. Phys., 11, 3527–3541, doi:10.5194/acp-11-3527-2011, 2011b. 3622
Köpke, P., Hess, M., Schult, I., and Shettle, E. P.: Global Aerosol Data Set, Max-Planck-Institut für Meteorologie Hamburg, Germany, 1997. 3622
Levin, Z., Ganor, E., and Gladstein, V.: The effects of desert particles coated with sulfate on rain formation in the Eastern Mediterranean, J. Appl. Meteorol., 35, 1511–1523, 1996. 3622
Lewandowski, P. A., Eichinger, W. E., Holder, H., Prueger, J., Wang, J., and Kleinman, L. I.: Vertical distribution of aerosols in the vicinity of Mexico City during MILAGRO-2006 Campaign, Atmos. Chem. Phys., 10, 1017–1030, doi:10.5194/acp-10-1017-2010, 2010. 3615

Lopatin, A., Dubovik, O., Chaikovsky, A., Goloub, P., Lapyonok, T., Tanré, D., and Litvinov, P.: Enhancement of aerosol characterization using synergy of lidar and sun-photometer coincident observations: the GARRLiC algorithm, Atmos. Meas. Tech., 6, 2065–2088, doi:10.5194/amt-6-2065-2013, 2013. 3610, 3615

Madonna, F., Amodeo, A., Boselli, A., Cornacchia, C., Cuomo, V., D'Amico, G., Giunta, A., Mona, L., and Pappalardo, G.: CIAO: the CNR-IMAA advanced observatory for atmospheric research, Atmos. Meas. Tech., 4, 1191–1208, doi:10.5194/amt-4-1191-2011, 2011. 3649

Madonna, F., Amato, F., Vande Hey, J., and Pappalardo, G.: Ceilometer aerosol profiling vs. Raman lidar in the frame of INTERACT campaign of ACTRIS, Atmos. Meas. Tech. Discuss., 7, 12407–12447, doi:10.5194/amtd-7-12407-2014, 2014. 3613

Mahowald, N. M., Kloster, S., Engelstaedter, S., Moore, J. K., Mukhopadhyay, S., McConnell, J. R., Albani, S., Doney, S. C., Bhattacharya, A., Curran, M. A. J., Flanner, M. G., Hoffman, F. M., Lawrence, D. M., Lindsay, K., Mayewski, P. A., Neff, J., Rothenberg, D., Thomas, E., Thornton, P. E., and Zender, C. S.: Observed 20th century desert dust variability: impact on climate and biogeochemistry, Atmos. Chem. Phys., 10, 10875–10893, doi:10.5194/acp-10-10875-2010, 2010. 3608

Mamouri, R. E. and Ansmann, A.: Fine and coarse dust separation with polarization lidar, Atmos. Meas. Tech., 7, 3717–3735, doi:10.5194/amt-7-3717-2014, 2014. 3615, 3620

Marticorena, B. and Bergametti, G.: Modeling the atmospheric dust cycle: 1. Design of a soil-derived dust emission scheme, J. Geophys. Res., 100, 16415–16430, doi:10.1029/95JD00690, 1995. 3618, 3647

Marticorena, B., Bergametti, G., Aumont, B., Callot, Y., N'Doumé, C., and Legrand, M.: Modeling the atmospheric dust cycle: 2. Simulation of Saharan dust sources, J. Geophys. Res., 102, 4387–4404, doi:10.1029/96JD02964, 1997. 3618

Matthias, V., Freudenthaler, V., Amodeo, A., Balin, I., Balis, D., Bösenberg, J., Chaikovsky, A., Chourdakis, G., Comeron, A., Delaval, A., De Tomasi, F., Eixmann, R., Hågård, A., Komguem, L., Kreipl, S., Matthey, R., Rizi, V., Rodrigues, J. A., Wandinger, U., and Wang, X.: Aerosol lidar intercomparison in the framework of the EARLINET project. 1. Instruments, Appl. Optics, 43, 961–976, 2004. 3612

Maurizi, A. and Monti, F.: DREAMABOL 1.0 – A BOLCHEM offspring for mineral dust, Geosci. Model Dev. Discuss., in preparation, 2015. 3617, 3647

Maurizi, A., D'Isidoro, M., and Mircea, M.: BOLCHEM: an integrated system for atmospheric dynamics and composition, in: Integrated Systems of Meso-Meteorological and Chemical

Transport Models, edited by: Baklanov, A., Alexander, M., and Sokhi, R., Springer, Berlin Heidelberg, 89–94, 2011. 3617
McArthur, L. J. B., Halliwell, D. H., Niebergall, O. J., O'Neill, N. T., Slusser, J. R., and Wehrli, C.: Field comparison of network Sun photometers, J. Geophys. Res., 108, 4596, doi:10.1029/2002JD002964, 2003. 3612
Mesinger, F.: A blocking technique for representation of mountains in atmospheric models, Riv. Meteorol. Aeronau., 44, 195–202, 1984. 3621
Mircea, M., D'Isidoro, M., Maurizi, A., Vitali, L., Monforti, F., Zanini, G., and Tampieri, F.: A comprehensive performance evaluation of the air quality model BOLCHEM to reproduce the ozone concentrations over Italy, Atmos. Environ., 42, 1169–1185, doi:10.1016/j.atmosenv.2007.10.043, 2008. 3617
Mona, L., Amodeo, A., Pandolfi, M., and Pappalardo, G.: Saharan dust intrusions in the Mediterranean area: three years of Raman lidar measurements, J. Geophys. Res., 111, D16203, doi:10.1029/2005JD006569, 2006. 3623, 3625, 3628
Mona, L., Liu, Z., Müller, D., Ller, D., Omar, A., Papayannis, A., Pappalardo, G., Sugimoto, N., and Vaughan, M.: Lidar measurements for desert dust characterization: an overview, Advances in Meteorology, 2012, e356265, doi:10.1155/2012/356265, 2012. 3613
Mona, L., Papagiannopoulos, N., Basart, S., Baldasano, J., Binietoglou, I., Cornacchia, C., and Pappalardo, G.: EARLINET dust observations vs. BSC-DREAM8b modeled profiles: 12-year-long systematic comparison at Potenza, Italy, Atmos. Chem. Phys., 14, 8781–8793, doi:10.5194/acp-14-8781-2014, 2014. 3609, 3623, 3628
Morman, S. A. and Plumlee, G. S.: Dust and human health, in: Mineral Dust, edited by: Knippertz, P. and Stuut, J.-B. W., Springer, Dordrecht, Netherlands, 385–409, 2014. 3608
Müller, D., Heinold, B., Tesche, M., Tegen, I., Althausen, D., Arboledas, L. A., Amiridis, V., Amodeo, A., Ansmann, A., Balis, D., Comeron, A., D'amico, G., Gerasopoulos, E., Guerrero-Rascado, J. L., Freudenthaler, V., Giannakaki, E., Heese, B., Iarlori, M., Knippertz, P., Mamouri, R. E., Mona, L., Papayannis, A., Pappalardo, G., Perrone, R.-M., Pisani, G., Rizi, V., Sicard, M., Spinelli, N., Tafuro, A., and Wiegner, M.: EARLINET observations of the 14–22-May long-range dust transport event during SAMUM 2006: validation of results from dust transport modelling, Tellus B, 61, 325–339, doi:10.3402/tellusb.v61i1.16832, 2009. 3609
Nemuc, A., Vasilescu, J., Talianu, C., Belegante, L., and Nicolae, D.: Assessment of aerosol's mass concentrations from measured linear particle depolarization ratio (vertically resolved)

AMTD
8, 3605–3666, 2015

Dust model comparison methodology

I. Binietoglou et al.

Title Page
Abstract Introduction
Conclusions References
Tables Figures
◀I ▶I
◀ ▶
Back Close
Full Screen / Esc
Printer-friendly Version
Interactive Discussion

and simulations, Atmos. Meas. Tech., 6, 3243–3255, doi:10.5194/amt-6-3243-2013, 2013. 3615, 3649

Nickovic, S. and Dobricic, S.: A model for long-range transport of desert dust, Mon. Weather Rev., 124, 2537–2544, 1996. 3616

Nickovic, S., Kallos, G., Papadopoulos, A., and Kakaliagou, O.: A model for prediction of desert dust cycle in the atmosphere, J. Geophys. Res., 106, 18113–18129, 2001. 3617, 3622, 3647

Nickovic, S., Vukovic, A., and Vujadinovic, M.: Atmospheric processing of iron carried by mineral dust, Atmos. Chem. Phys., 13, 9169–9181, doi:10.5194/acp-13-9169-2013, 2013. 3608

Papayannis, A., Balis, D., Amiridis, V., Chourdakis, G., Tsaknakis, G., Zerefos, C., Castanho, A. D. A., Nickovic, S., Kazadzis, S., and Grabowski, J.: Measurements of Saharan dust aerosols over the Eastern Mediterranean using elastic backscatter-Raman lidar, spectrophotometric and satellite observations in the frame of the EARLINET project, Atmos. Chem. Phys., 5, 2065–2079, doi:10.5194/acp-5-2065-2005, 2005. 3613

Papayannis, A., Amiridis, V., Mona, L., Tsaknakis, G., Balis, D., Bösenberg, J., Chaikovski, A., De Tomasi, F., Grigorov, I., Mattis, I., Mitev, V., Müller, D., Nickovic, S., Pérez, C., Pietruczuk, A., Pisani, G., Ravetta, F., Rizi, V., Sicard, M., Trickl, T., Wiegner, M., Gerding, M., Mamouri, R. E., D'Amico, G., and Pappalardo, G.: Systematic lidar observations of Saharan dust over Europe in the frame of EARLINET (2000–2002), J. Geophys. Res., 113, D10204, doi:doi:10.1029/2007JD009028, 2008. 3625

Papayannis, A., Balis, D., Kokkalis, P., Mamouri, R., Tsaknakis, G., Giannakaki, E., Siomos, N., and Amiridis, V.: ARIADNE: the Greek lidar network, Proceedings, 26th International Laser Radar Conference, Porto Heli, Greece, 349–352, 2012. 3649

Pappalardo, G., Amodeo, A., Pandolfi, M., Wandinger, U., Ansmann, A., Bösenberg, J., Matthias, V., Amiridis, V., De Tomasi, F., Frioud, M., Iarlori, M., Komguem, L., Papayannis, A., Rocadenbosch, F., and Wang, X.: Aerosol lidar intercomparison in the framework of the EARLINET project. 3. Raman lidar algorithm for aerosol extinction, backscatter, and lidar ratio, Appl. Optics, 43, 5370–5385, 2004. 3612, 3621

Pappalardo, G., Amodeo, A., Apituley, A., Comeron, A., Freudenthaler, V., Linné, H., Ansmann, A., Bösenberg, J., D'Amico, G., Mattis, I., Mona, L., Wandinger, U., Amiridis, V., Alados-Arboledas, L., Nicolae, D., and Wiegner, M.: EARLINET: towards an advanced sustainable European aerosol lidar network, Atmos. Meas. Tech., 7, 2389–2409, doi:10.5194/amt-7-2389-2014, 2014. 3611, 3612

Pay, M. T., Piot, M., Jorba, O., Gassó, S., Gonçalves, M., Basart, S., Dabdub, D., Jiménez-Guerrero, P., and Baldasano, J. M.: A full year evaluation of the CALIOPE-EU air quality modeling system over Europe for 2004, Atmos. Environ., 44, 3322–3342, doi:10.1016/j.atmosenv.2010.05.040, 2010. 3617

Perrone, M. R., De Tomasi, F., and Gobbi, G. P.: Vertically resolved aerosol properties by multi-wavelength lidar measurements, Atmos. Chem. Phys., 14, 1185–1204, doi:10.5194/acp-14-1185-2014, 2014. 3649

Pietruczuk, A. and Chaikovsky, A.: Variability of aerosol properties during the 2007–2010 spring seasons over central Europe, Acta Geophys., 60, 1338–1358, doi:10.2478/s11600-012-0017-9, 2012. 3649

Preißler, J., Wagner, F., Pereira, S. N., and Guerrero-Rascado, J. L.: Multi-instrumental observation of an exceptionally strong Saharan dust outbreak over Portugal, J. Geophys. Res., 116, D24204, doi:10.1029/2011JD016527, 2011. 3649

Pérez, C., Nickovic, S., Baldasano, J. M., Sicard, M., Rocadenbosch, F., and Cachorro, V. E.: A long Saharan dust event over the western Mediterranean: lidar, Sun photometer observations, and regional dust modeling, J. Geophys. Res.-Atmos., 111, D15214, 2006a. 3609, 3617, 3618

Pérez, C., Nickovic, S., Pejanovic, G., Baldasano, J. M., and Özsoy, E.: Interactive dust-radiation modeling: a step to improve weather forecasts, J. Geophys. Res., 111, D16206, doi:10.1029/2005JD006717, 2006b. 3608, 3617

Pérez, C., Haustein, K., Janjic, Z., Jorba, O., Huneeus, N., Baldasano, J. M., Black, T., Basart, S., Nickovic, S., Miller, R. L., Perlwitz, J. P., Schulz, M., and Thomson, M.: Atmospheric dust modeling from meso to global scales with the online NMMB/BSC-Dust model – Part 1: Model description, annual simulations and evaluation, Atmos. Chem. Phys., 11, 13001–13027, doi:10.5194/acp-11-13001-2011, 2011. 3609, 3618

Rocadenbosch, F., Frasier, S., Kumar, D., Lange, D., Gregorio, E., and Sicard, M.: Backscatter error bounds for the elastic lidar two-component inversion algorithm, IEEE T. Geosci. Remote, 50, 4791–4803, doi:10.1109/TGRS.2012.2194501, 2012. 3613

Rosenfeld, D., Rudich, Y., and Lahav, R.: Desert dust suppressing precipitation: a possible desertification feedback loop, P. Natl. Acad. Sci. USA, 98, 5975–5980, doi:10.1073/pnas.101122798, 2001. 3608

Schulz, M., Balkanski, Y. J., Guelle, W., and Dulac, F.: Role of aerosol size distribution and source location in a three-dimensional simulation of a Saharan dust episode tested against satellite-derived optical thickness, J. Geophys. Res., 103, 10579–10592, doi:10.1029/97JD02779, 1998. 3618

Seigneur, C., Pun, B., Pai, P., Louis, J.-F., Solomon, P., Emery, C., Morris, R., Zahniser, M., Worsnop, D., and Koutrakis, P.: Guidance for the performance evaluation of three-dimensional air quality modeling systems for particulate matter and visibility, J. Air Waste Manage., 50, 588–599, 2000. 3619

Sekiyama, T. T., Tanaka, T. Y., Shimizu, A., and Miyoshi, T.: Data assimilation of CALIPSO aerosol observations, Atmos. Chem. Phys., 10, 39–49, doi:10.5194/acp-10-39-2010, 2010. 3609

Shao, Y., Raupach, M. R., and Findlater, P. A.: Effect of saltation bombardment on the entrainment of dust by wind, J. Geophys. Res., 98, 12719–12726, doi:10.1029/93JD00396, 1993. 3647

Shettle, E. P.: Optical and radiative properties of a desert aerosol model, in: International Radiation Symposium on Current Problems in Atmospheric Radiation, 21-28 August 1984, Perugia, Italy, 1986. 3618

Shimizu, A., Sugimoto, N., Matsui, I., Arao, K., Uno, I., Murayama, T., Kagawa, N., Aoki, K., Uchiyama, A., and Yamazaki, A.: Continuous observations of Asian dust and other aerosols by polarization lidars in China and Japan during ACE-Asia, J. Geophys. Res., 109, D19S17, doi:10.1029/2002JD003253, 2004. 3613

Sicard, M., D'Amico, G., Comerón, A., Alados-Arboledas, L., Amodeo, A., Baars, H., Belegante, L., Binietoglou, I., Bravo-Aranda, J. A., Christodoulou, A., Fernández, A., Fréville, P., Garcia-Vizcaino, D., Giunta, A., Granados-Muñoz, M. J., Guerrero-Rascado, J. L., Hadjimitsis, D., Haefele, A., Hervo, M., Iarlori, M., Kokkalis, P., Lange, D., Mamouri, R., Mattis, I., Molero, F., Mona, L., Montoux, N., Muñoz, A., Muñoz Porcar, C., Nicolae, D., Nisantzi, A., Papayannis, A., Pappalardo, G., Pereira, S. N., Preißler, J., Pujadas, M., Rizi, V., Rocadenbosch, F., Sellegri, K., Simeonov, V., Tsaknakis, G., and Wagner, F.: EARLINET: potential operationality of a research network, Atmos. Meas. Tech. Discuss., in preparation, 2015. 3619

Simmons, A. J. and Burridge, D. M.: An energy and angular-momentum conserving vertical finite-difference scheme and hybrid vertical coordinates, Mon. Weather Rev., 109, 758–766, 1981. 3621

Sokolik, I. N. and Toon, O. B.: Direct radiative forcing by anthropogenic airborne mineral aerosols, Nature, 381, 681–683, 1996. 3608

Solomos, S., Kallos, G., Kushta, J., Astitha, M., Tremback, C., Nenes, A., and Levin, Z.: An integrated modeling study on the effects of mineral dust and sea salt particles on clouds and precipitation, Atmos. Chem. Phys., 11, 873–892, doi:10.5194/acp-11-873-2011, 2011. 3608
Sugimoto, N., Shimizu, A., Matsui, I., Uno, I., Arao, K., Dong, X., Zhao, S., Zhou, J., and Lee, C.-H.: Study of Asian dust phenomena in 2001–2003 using a network of continuously operated polarization lidars, Water Air Soil Poll., 5, 145–157, 2005. 3611
Takamura, T. and Nakajima, T.: Overview of SKYNET and its activities, Optica pura y aplicada, 37, 3303–3308, 2004. 3612
Taylor, K. E.: Summarizing multiple aspects of model performance in a single diagram, J. Geophys. Res.-Atmos., 106, 7183–7192, doi:10.1029/2000JD900719, 2001. 3628
Tegen, I.: Modeling the mineral dust aerosol cycle in the climate system, Quaternary Sci. Rev., 22, 1821–1834, doi:10.1016/S0277-3791(03)00163-X, 2003. 3608
Tegen, I. and Fung, I.: Modeling of mineral dust in the atmosphere: sources, transport, and optical thickness, J. Geophys. Res., 99, 22897–22914, 1994. 3616, 3622
Tegen, I. and Lacis, A. A.: Modeling of particle size distribution and its influence on the radiative properties of mineral dust aerosol, J. Geophys. Res., 101, 19237–19244, doi:10.1029/95JD03610, 1996. 3618
Tesche, M., Ansmann, A., Müller, D., Althausen, D., Engelmann, R., Freudenthaler, V., and Groß, S.: Vertically resolved separation of dust and smoke over Cape Verde using multiwavelength Raman and polarization lidars during Saharan Mineral Dust Experiment 2008, J. Geophys. Res.-Atmos., 114, D13202, doi:10.1029/2009JD011862, 2009. 3614
The EARLINET publishing group 2000–2010, Adam, M., Alados-Arboledas, L., Althausen, D., Amiridis, V., Amodeo, A., Ansmann, A., Apituley, A., Arshinov, Y., Balis, D., Belegante, L., Bobrovnikov, S., Boselli, A., Bravo-Aranda, J. A., Bösenberg, J., Carstea, E., Chaikovsky, A., Comerón, A., D'Amico, G., Daou, D., Dreischuh, T., Engelmann, R., Finger, F., Freudenthaler, V., Garcia-Vizcaino, D., García, A. J. F., Geiß, A., Giannakaki, E., Giehl, H., Giunta, A., de Graaf, M., Granados-Muñoz, M. J., Grein, M., Grigorov, I., Groß, S., Gruening, C., Guerrero-Rascado, J. L., Haeffelin, M., Hayek, T., Iarlori, M., Kanitz, T., Kokkalis, P., Linné, H., Madonna, F., Mamouriat, R.-E., Matthias, V., Mattis, I., Menéndez, F. M., Mitev, V., Mona, L., Morille, Y., Muñoz, C., Müller, A., Müller, D., Navas-Guzmán, F., Nemuc, A., Nicolae, D., Pandolfi, M., Papayannis, A., Pappalardo, G., Pelon, J., Perrone, M. R., Pietruczuk, A., Pisani, G., Potma, C., Preißler, J., Pujadas, M., Putaud, J., Radu, C., Ravetta, F., Reigert, A., Rizi, V., Rocadenbosch, F., Rodríguez, A., Sauvage, L., Schmidt, J.,

AMTD
8, 3605–3666, 2015

Dust model comparison methodology

I. Binietoglou et al.

Schnell, F., Schwarz, A., Seifert, P., Serikov, I., Sicard, M., Silva, A. M., Simeonov, V., Siomos, N., Sirch, T., Spinelli, N., Stoyanov, D., Talianu, C., Tesche, M., De Tomasi, F., Trickl, T., Vaughan, G., Volten, H., Wagner, F., Wandinger, U., Wang, X., Wiegner, M., and Wilson, K. M. A.: EARLINET All Observations (2000–2010), World Data Center for Climate (WDCC), doi:10.1594/WDCC/EN_all_measurements_2000-2010, 2014. 3612

Todd, M. C., Washington, R., Martins, J. V., Dubovik, O., Lizcano, G., M'bainayel, S., and Engelstaedter, S.: Mineral dust emission from the Bodélé Depression, northern Chad, during BoDEx 2005, J. Geophys. Res., 112, D06207, doi:doi:10.1029/2006JD007170, 2007. 3622

Tsekeri, A., Amiridis, V., Kokkalis, P., Basart, S., Chaikovsky, A., Dubovik, O., Papayannis, R., and Baldasano, J. M.: Application of a synergetic lidar and sunphotometer algorithm for the characterization of a dust event over Athens, Greece, British Journal of Environment and Climate Change, 3, 531–546, 2013. 3610

Uno, I., Wang, Z., Chiba, M., Chun, Y. S., Gong, S. L., Hara, Y., Jung, E., Lee, S.-S., Liu, M., Mikami, M., Music, S., Nickovic, S., Satake, S., Shao, Y., Song, Z., Sugimoto, N., Tanaka, T., and Westphal, D. L.: Dust model intercomparison (DMIP) study over Asia: overview, J. Geophys. Res., 111, D12213, doi:10.1029/2005JD006575, 2006. 3609

Wagner, J., Ansmann, A., Wandinger, U., Seifert, P., Schwarz, A., Tesche, M., Chaikovsky, A., and Dubovik, O.: Evaluation of the Lidar/Radiometer Inversion Code (LIRIC) to determine microphysical properties of volcanic and desert dust, Atmos. Meas. Tech., 6, 1707–1724, doi:10.5194/amt-6-1707-2013, 2013. 3616

Wang, Y., Sartelet, K. N., Bocquet, M., Chazette, P., Sicard, M., D'Amico, G., Léon, J. F., Alados-Arboledas, L., Amodeo, A., Augustin, P., Bach, J., Belegante, L., Binietoglou, I., Bush, X., Comerón, A., Delbarre, H., García-Vízcaino, D., Guerrero-Rascado, J. L., Hervo, M., Iarlori, M., Kokkalis, P., Lange, D., Molero, F., Montoux, N., Muñoz, A., Muñoz, C., Nicolae, D., Papayannis, A., Pappalardo, G., Preissler, J., Rizi, V., Rocadenbosch, F., Sellegri, K., Wagner, F., and Dulac, F.: Assimilation of lidar signals: application to aerosol forecasting in the western Mediterranean basin, Atmos. Chem. Phys., 14, 12031–12053, doi:10.5194/acp-14-12031-2014, 2014. 3609, 3619

White, B. R.: Soil transport by winds on Mars, J. Geophys. Res., 84, 4643–4651, doi:10.1029/JB084iB09p04643, 1979. 3618, 3647

Wiegner, M., Madonna, F., Binietoglou, I., Forkel, R., Gasteiger, J., Geiß, A., Pappalardo, G., Schäfer, K., and Thomas, W.: What is the benefit of ceilometers for aerosol remote sensing?

an answer from EARLINET, Atmos. Meas. Tech., 7, 1979–1997, doi:10.5194/amt-7-1979-2014, 2014. 3613
Yumimoto, K., Uno, I., Sugimoto, N., Shimizu, A., Hara, Y., and Takemura, T.: Size-resolved adjoint inversion of Asian dust, Geophys. Res. Lett., 39, L24808, doi:10.1029/2012GL053890, 2012. 3622
Zender, C. S., Bian, H., and Newman, D.: Mineral Dust Entrainment and Deposition (DEAD) model: description and 1990s dust climatology, J. Geophys. Res., 108, 4416, doi:10.1029/2002JD002775, 2003. 3618
Zhang, L., Gong, S., Padro, J., and Barrie, L.: A size-segregated particle dry deposition scheme for an atmospheric aerosol module, Atmos. Environ., 35, 549–560, doi:10.1016/S1352-2310(00)00326-5, 2001. 3647

AMTD
8, 3605–3666, 2015
Dust model comparison methodology
I. Binietoglou et al.

Table 1. Comparison of lidar dust products for dust model evaluation.

Product	Geometrical properties	Quantitative	Mixed dust cases	Direct comparison
Range corrected signals	Yes	No	No	No
Optical products	Yes	Yes	No	No
Dust optical products	Yes	Yes	Yes	No
Dust concentration	Yes	Yes	Yes	Yes

AMTD
8, 3605–3666, 2015

Table 2. Summary of the main parameters of the dust transport models used in this study (adapted from Benedetti et al., 2014).

	BSC-DREAM8b v2	NMMB/BSC-DUST	DREAMABOL	DREAM8-NMME-MACC
Institution	BSC-CNS	BSC-CNS	CNR-ISAC	SEEVCCC
Meteorological driver	Eta/NCEP	NMMB/NCEP	BOLAM	NMME/NCEP
Initial and boundary conditions	NCEP/GFS	NCEP/GFS	NCEP/GFS	ECMWF
Resolution	0.33° × 0.33°	0.33° × 0.33°	0.4° × 0.4°	0.25° × 0.25°
Source mask	USGS-FAO with Ginoux et al. (2001)	USGS-FAO with Ginoux et al. (2001)	USGS-FAO with Ginoux et al. (2001)	USGS-FAO with Ginoux et al. (2001)
Emission scheme	Uplifting –Shao et al. (1993) –Janjic (1994) –Nickovic et al. (2001)	Saltation and sandblasting –White (1979) –Marticorena and Bergametti (1995) –Janjic (1994) –Nickovic et al. (2001)	Uplifting –Shao et al. (1993) –Nickovic et al. (2001)	Uplifting –Shao et al. (1993) –Janjic (1994) –Nickovic et al. (2001)
Deposition scheme	Dry deposition –Zhang et al. (2001) Below-cloud scavenging –Nickovic et al. (2001)	Dry deposition –Zhang et al. (2001) Wet deposition –Ferrier et al. (2002) –Betts (1986) –Janjic (1994)	Dry deposition –Zhang et al. (2001) In and below-cloud scavenging –Maurizi and Monti (2015) Convective clouds, precipitation and re-evaporation	Dry deposition –Zhang et al. (2001) Below-cloud scavenging –Nickovic et al. (2001)
Vertical resolution	24 Eta-layers	40 σ-hybrid layers	50 σ-hybrid layers	24 σ-hybrid layers
Transport size bins	8 (0.1–10 µm)	8 (0.1–10 µm)	8 (0.1–10 µm)	8 (0.1–10 µm)
Radiation interaction	Yes	No	No	No
Data assimilation	No	No	No	Yes

AMTD
8, 3605–3666, 2015

Title Page
Abstract Introduction
Conclusions References
Tables Figures
Back Close
Full Screen / Esc
Printer-friendly Version
Interactive Discussion

Table 3. Definition, symbol, value range, and ideal score for the statistical performance indicators used in the systematic examination of dust model concentration profiles. c denotes the concentration at altitude z. M_i and O_i represent modeled and observed profiles, respectively for the ith measurement pair. Altitude dependence is omitted for brevity.

Metric	Symbol	Definition	Range	Perfect score
Center of mass	CoM	$\frac{\int_{z_{\min}}^{z_{\max}} z \cdot c \cdot \mathrm{d}z}{\int_{z_{\min}}^{z_{\max}} c \cdot \mathrm{d}z}$	–	–
Mean Bias	MB	$\frac{1}{N}\sum_{i=1}^{N}(M_i - O_i)$	$-\infty$–∞	0
Correlation coefficient	r	$\frac{\sum_{i=1}^{N}\left(M_i-\overline{M}\right)\left(O_i-\overline{O}\right)}{\left[\sum_{i=1}^{N}\left(M_i-\overline{M}\right)^2\sum_{i=1}^{N}\left(O_i-\overline{O}\right)^2\right]^{\frac{1}{2}}}$	−1–1	1
Root Mean Square Error	RMSE	$\left[\frac{1}{N}\sum_{i=1}^{N}(M_i - O_i)^2\right]^{\frac{1}{2}}$	0–∞	0
Fractional Bias	F_{B}	$\frac{2}{N}\sum_{i=1}^{N}\left(\frac{M_i-O_i}{M_i+O_i}\right)$	−2–2	0
Fractional Gross Error	F_{E}	$\frac{2}{N}\sum_{i=1}^{N}\left\lvert\frac{M_i-O_i}{M_i+O_i}\right\rvert$	0–2	0

AMTD
8, 3605–3666, 2015

Table 4. The following 10 stations provided dust concentration profiles retrieved by the LIRIC algorithm. Three measurements of the Evora station do not include depolarization information. The provided references give further information for each station and the measurement instruments.

Station	Location (° N, ° E)	Altitude (m)	Lidar channels	No. Profiles	Reference
Athens	37.97, 23.77	212	3β	3	Kokkalis et al. (2012)
Barcelona	41.39, 2.17	115	3β	8	Kumar et al. (2011a)
Belsk	51.84, 20.79	180	3β	1	Pietruczuk and Chaikovsky (2012)
Bucharest	44.35, 26.03	93	$3\beta + 1\delta$	5	Nemuc et al. (2013)
Evora	38.57, −7.91	293	$3\beta + 1\delta^*$	18	Preißler et al. (2011)
Granada	37.16, −3.61	680	$3\beta + 1\delta$	8	Guerrero-Rascado et al. (2009)
Lecce	40.30, 18.10	30	$3\beta + 1\delta$	4	Perrone et al. (2014)
Leipzig	51.35, 12.43	90	$3\beta + 1\delta$	3	Althausen et al. (2009)
Potenza	40.60, 15.72	760	$3\beta + 1\delta$	8	Madonna et al. (2011)
Thessaloniki	40.63, 22.95	60	3β	3	Papayannis et al. (2012)

AMTD
8, 3605–3666, 2015

Table 5. Correlation coefficient (r) and fractional bias (F_B) for single value metrics of the compared profiles.

	Center of Mass		Total concentration		Peak value	
	r	F_B	r	F_B	r	F_B
BSC-DREAM8b v2	0.60	0.01	0.74	−0.90	0.69	−0.88
NMMB/BSC-DUST	0.79	0.16	0.82	−0.76	0.70	−0.76
DREAMABOL	0.72	0.01	0.52	−1.05	0.52	−0.89
DREAM8-NMME-MACC	0.79	0.13	0.77	−0.25	0.72	−0.31

AMTD
8, 3605–3666, 2015

Dust model comparison methodology

I. Binietoglou et al.

Figure 1. Map of the ACTRIS/EARLINET remote sensing stations providing data for testing the proposed methodology.

AMTD
8, 3605–3666, 2015

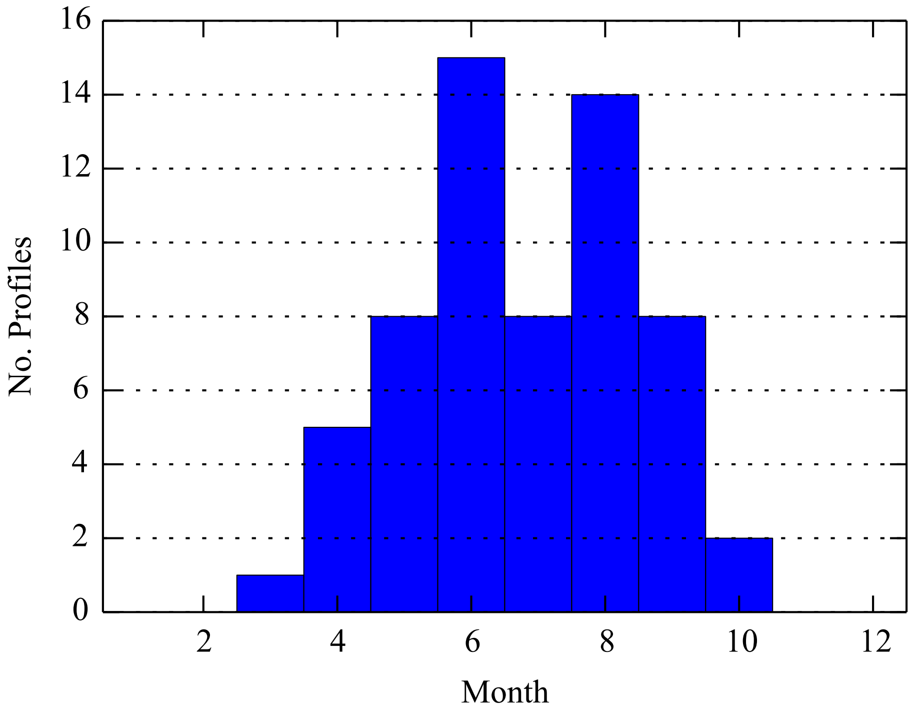

Figure 2. Distribution of available measurements per month.

AMTD
8, 3605–3666, 2015

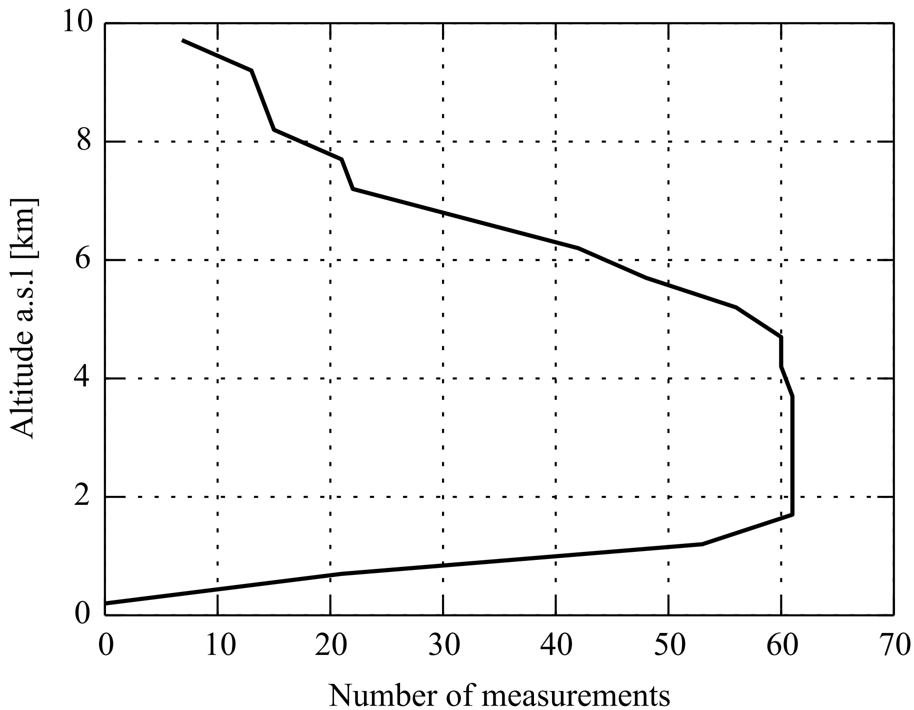

Figure 3. Number of used remote sensing profiles per altitude.

AMTD
8, 3605–3666, 2015

Dust model comparison methodology

I. Binietoglou et al.

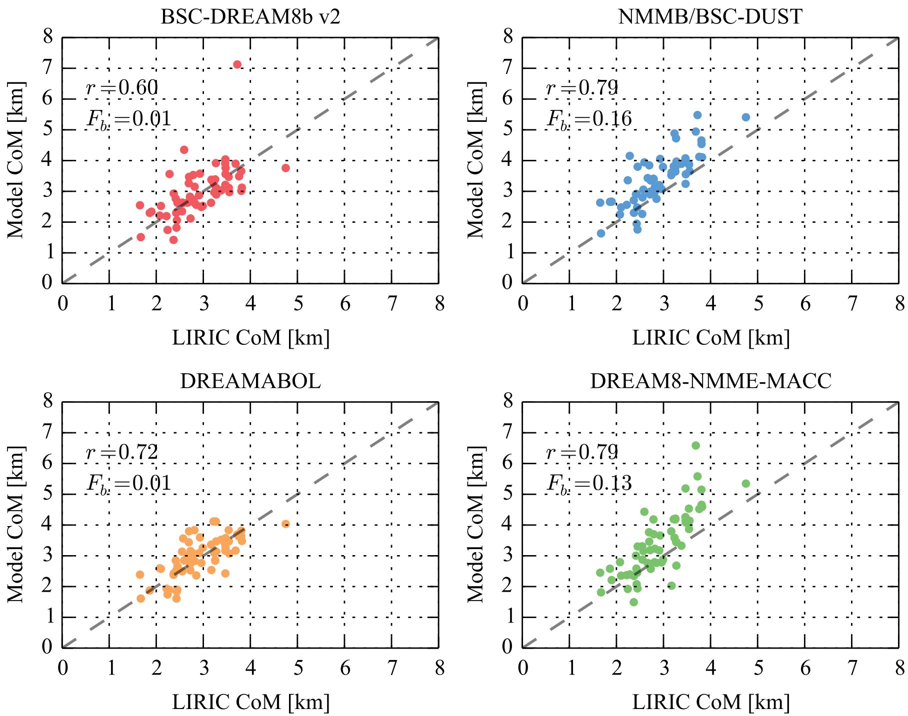

Figure 4. Comparison of dust center of mass for the four models against the ones retrieved from LIRIC.

AMTD
8, 3605–3666, 2015

I. Binietoglou et al.

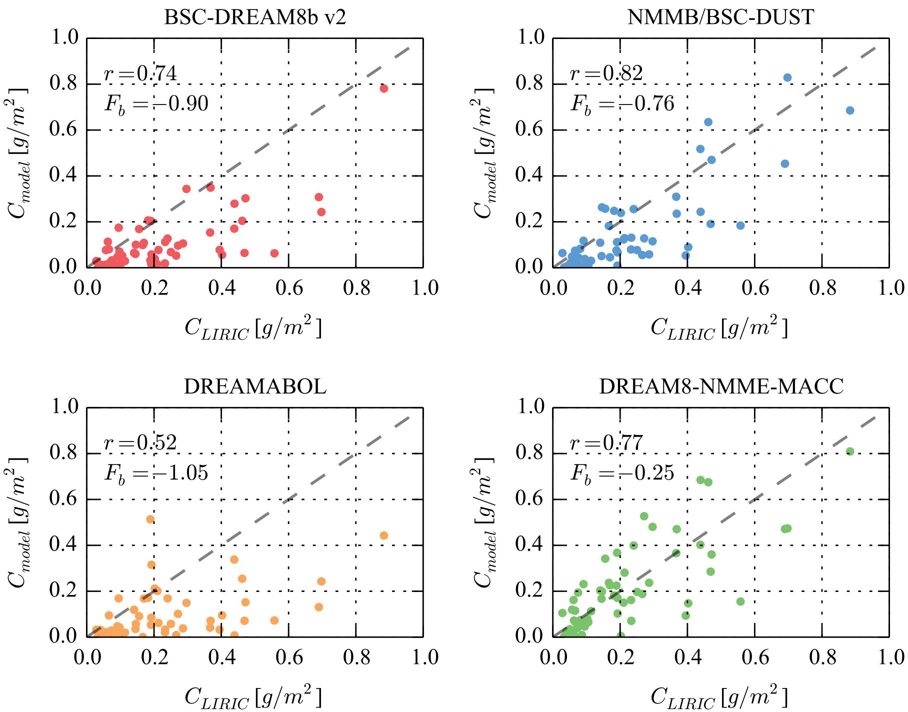

Figure 5. Comparison of integrated dust concentration for the four models against the ones retrieved from LIRIC. The value is calculated only for the altitude ranges for which both models and measurements provide valid values.

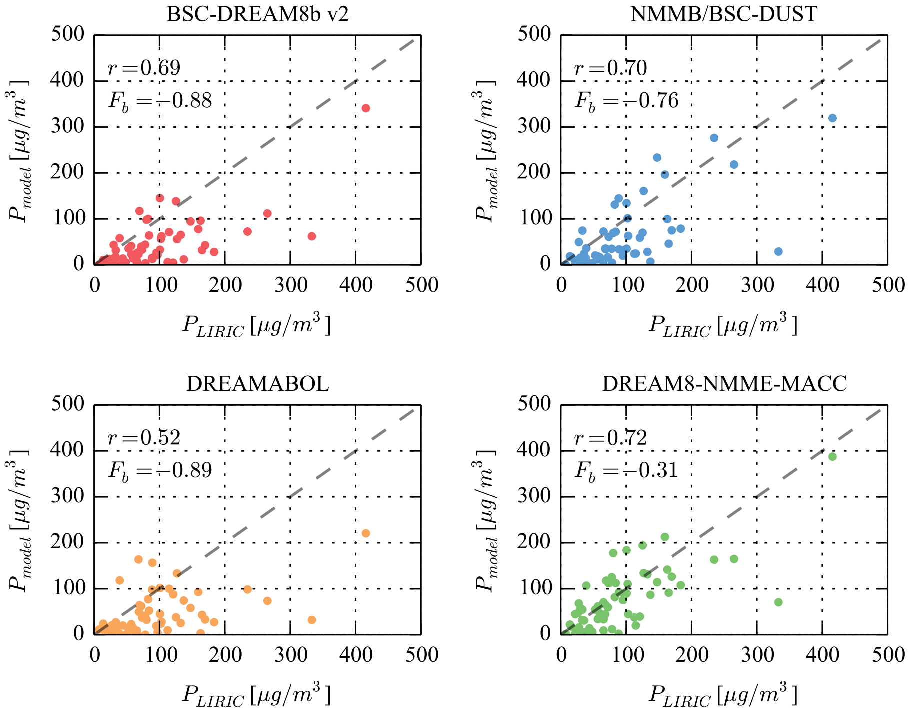

Figure 6. Comparison of profile peak value for the four models against the ones retrieved from LIRIC.

AMTD
8, 3605–3666, 2015

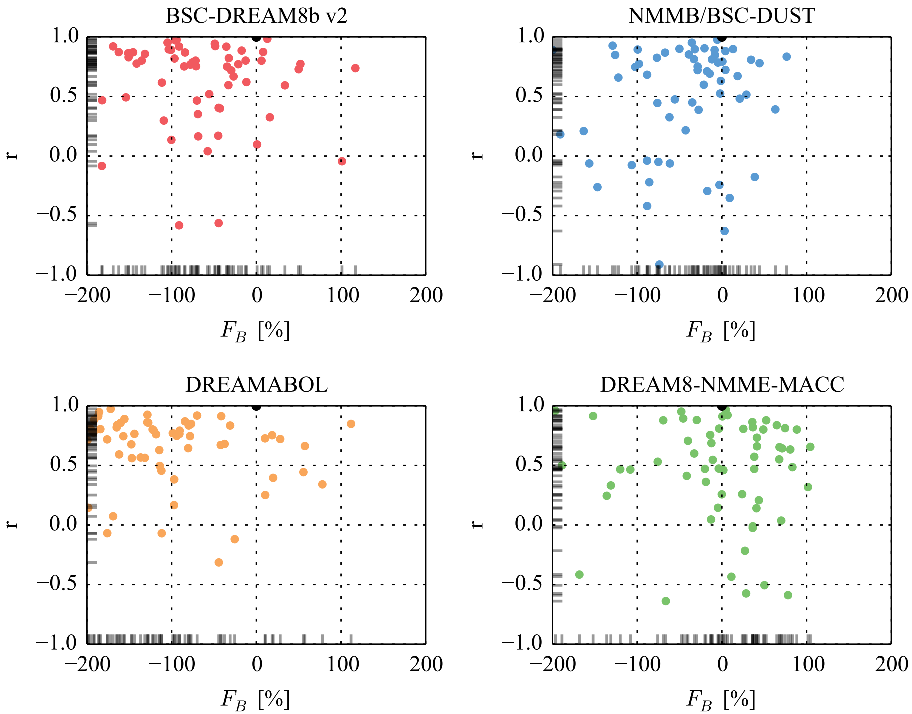

Figure 7. Scatter plot of vertical correlation and fractional gross error. Black dots represent the ideal performance (0, 1). Each point on the plot corresponds to a pair consisting of one LIRIC and one model profile.The bars on the axis indicate the univariate distribution of the data for each variable.

AMTD
8, 3605–3666, 2015

Dust model comparison methodology

I. Binietoglou et al.

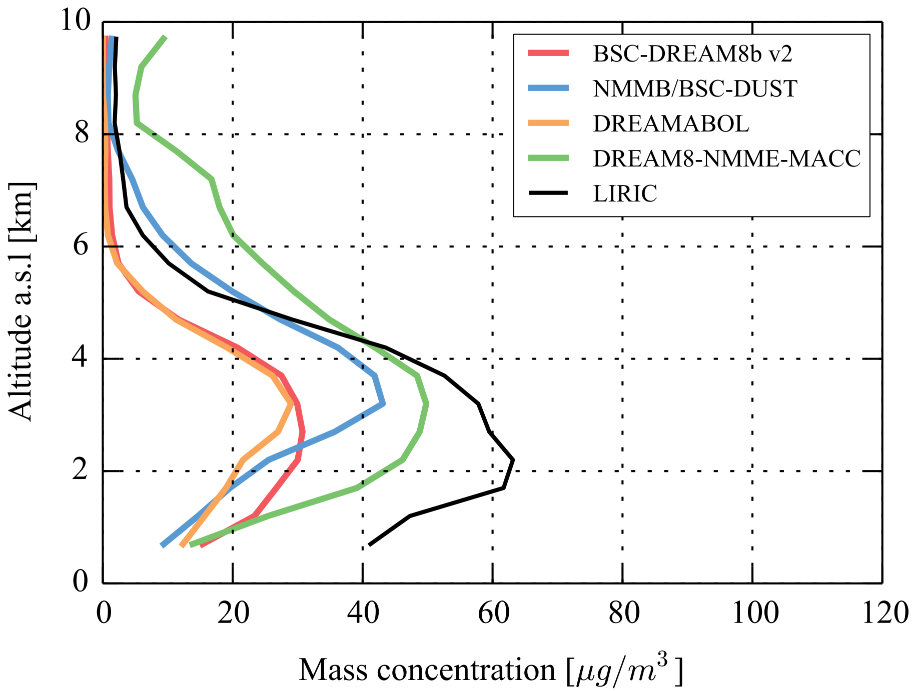

Figure 8. Average profile comparison as simulated by four model and retrieved by LIRIC.

AMTD
8, 3605–3666, 2015

Dust model comparison methodology

I. Binietoglou et al.

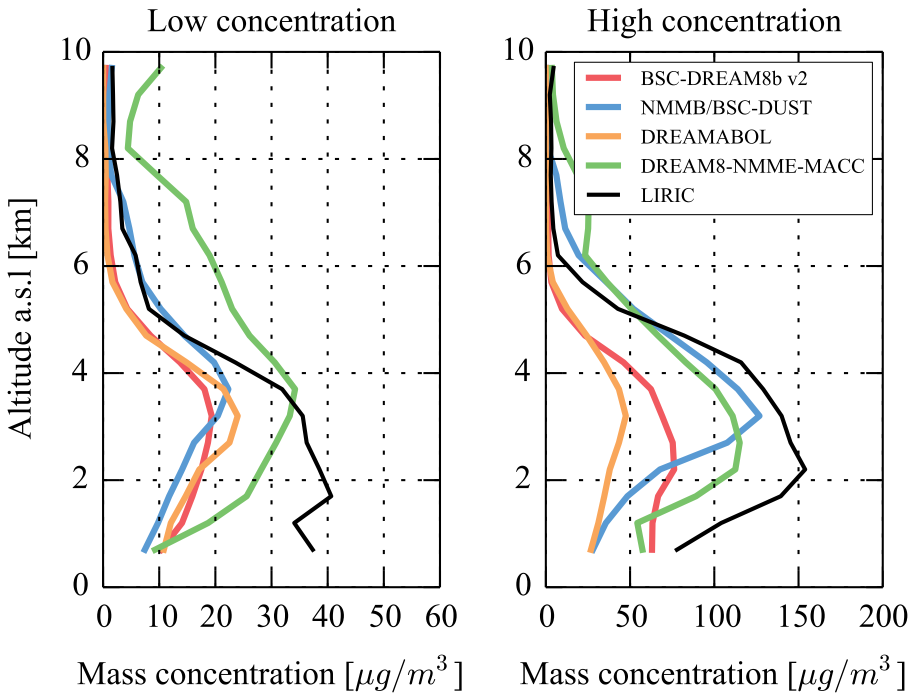

Figure 9. Comparison of average profiles simulated by all four model for low and high concentration cases, separated at 0.3 g m^{-2}.

AMTD
8, 3605–3666, 2015

Dust model comparison methodology

I. Binietoglou et al.

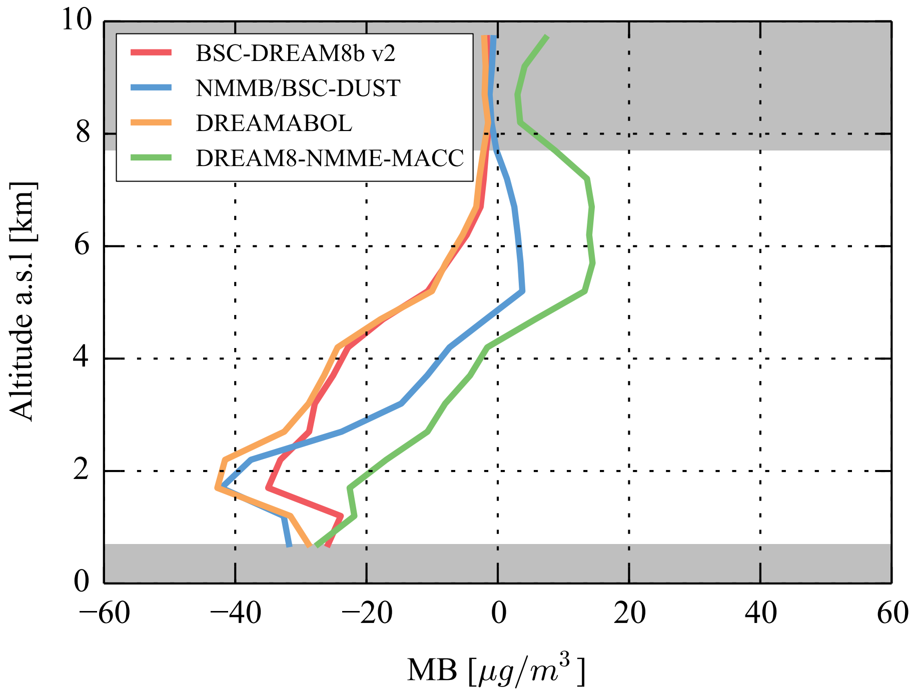

Figure 10. Profiles of mean bias error for all four models. Gray shading indicates altitude ranges with less than 20 profiles available.

AMTD
8, 3605–3666, 2015

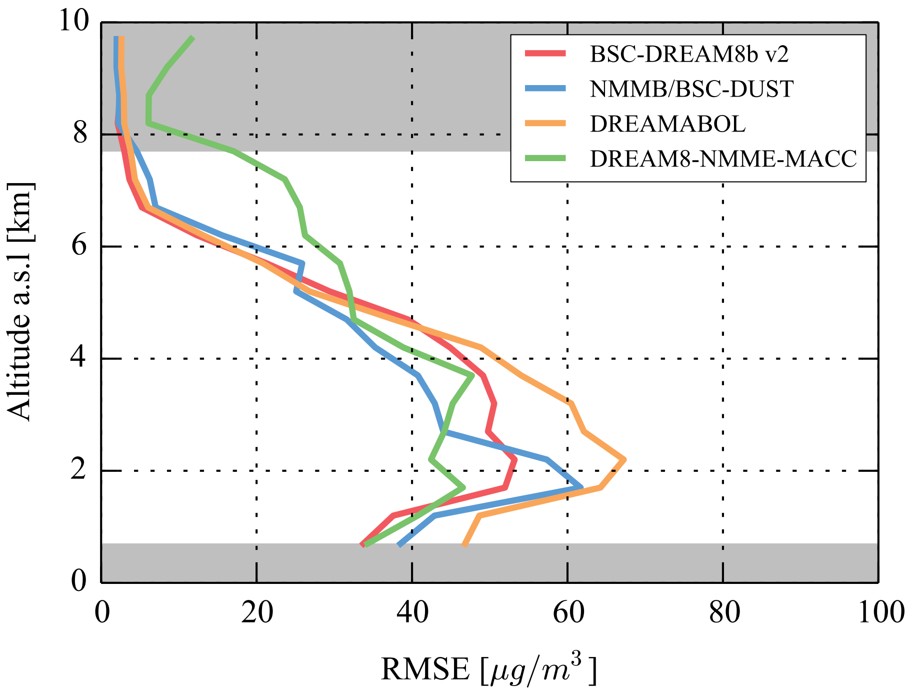

Figure 11. Profiles of root mean square error for all four models. Gray shading indicates altitude ranges with less than 20 profiles available.

AMTD
8, 3605–3666, 2015

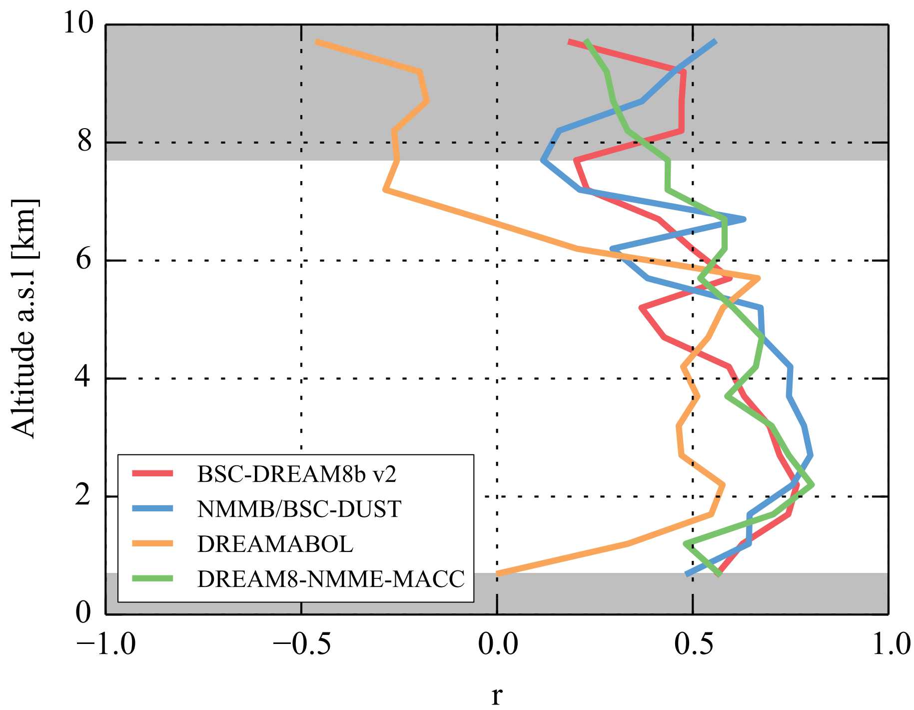

Figure 12. Profiles of correlation coefficient *r* for all four models. Gray shading indicates altitude ranges with less than 20 profiles available.

AMTD
8, 3605–3666, 2015

Dust model comparison methodology

I. Binietoglou et al.

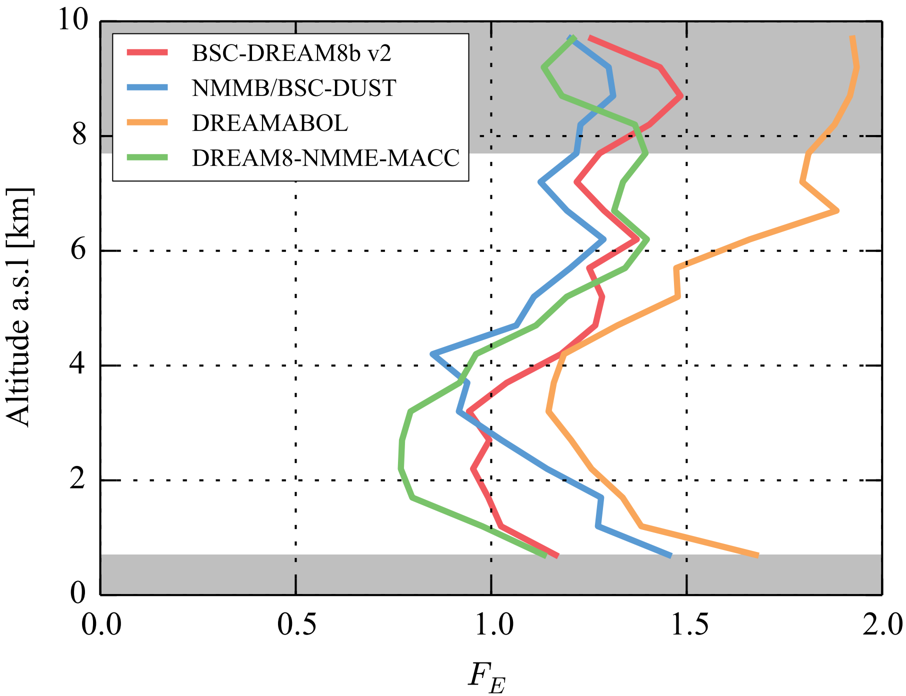

Figure 13. Profiles of fractional gross error *r* for all four models. Gray shading indicates altitude ranges with less than 20 profiles available.

AMTD
8, 3605–3666, 2015

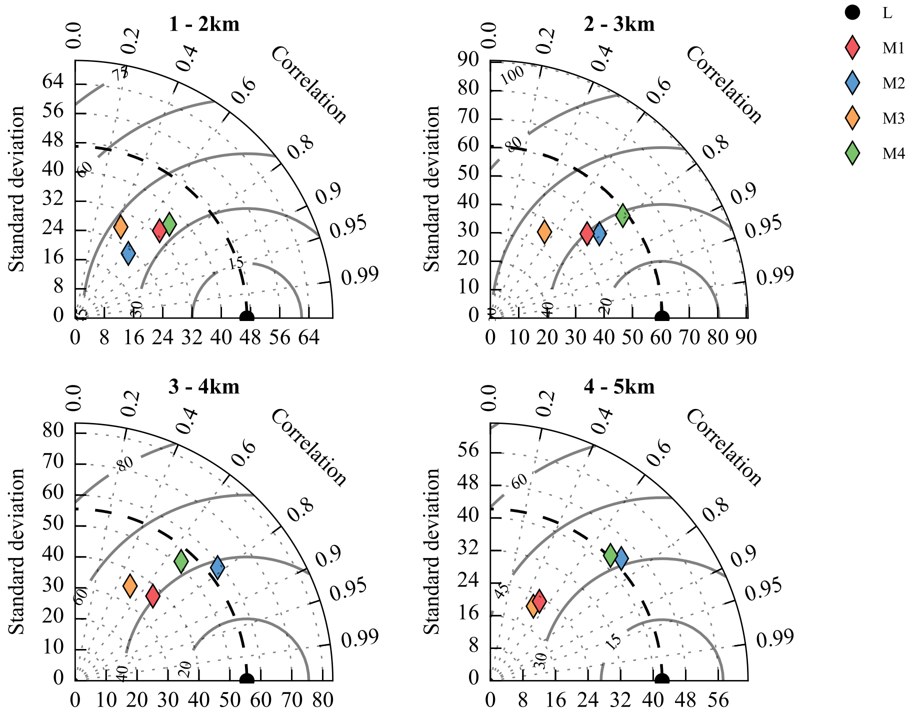

Figure 14. Taylor's diagrams for four different altitude ranges, from 1 to 5 km. The black dots represent the observational data. The distance of any point from the origin indicates the SD of the dataset. The angular distance of a point from the horizontal axis indicates the correlation of model and measured data. The distance of two points in these plots is proportional to their centered root mean square (RMS) difference. L: LIRIC observations, M1: BSC-DREAM8b v2, M2: NMMB/BSC-DUST, M3: DREAMBOL, M4: DREAM8-NMME-MACC.

AMTD
8, 3605–3666, 2015

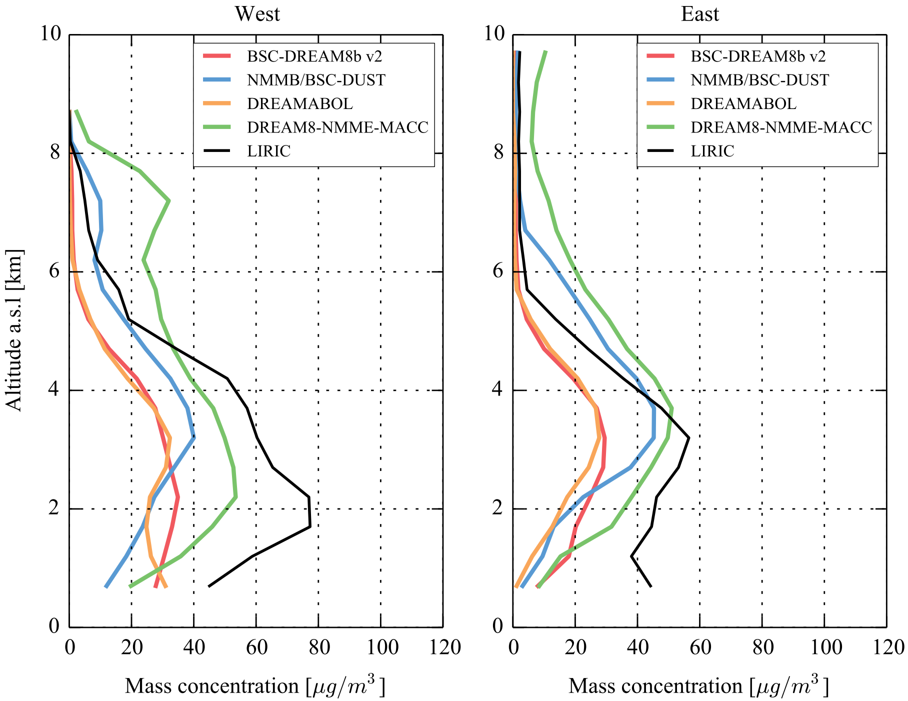

Figure 15. Comparison of mean concentration profiles for the west and east station clusters.

AMTD
8, 3605–3666, 2015

Dust model comparison methodology

I. Binietoglou et al.

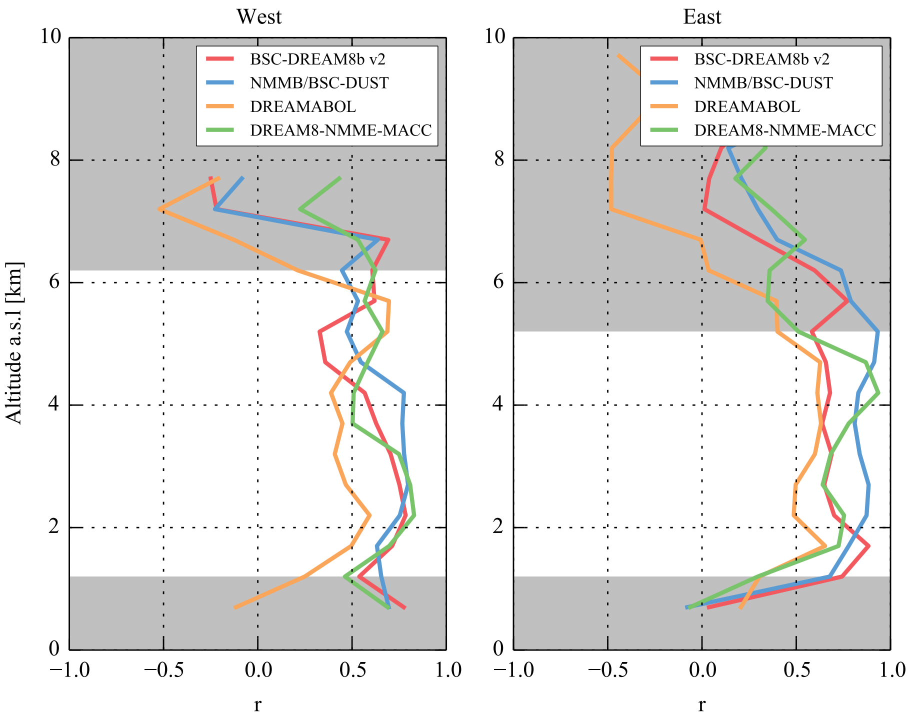

Figure 16. Comparison of correlation coefficient profiles for the west and east station clusters. Gray shading indicates altitude ranges with less than 20 profiles available.

AMTD
8, 3605–3666, 2015